Trace element proxies and stable isotopes used to identify water quality threats to elkhorn coral (*Acropora palmata)* at two national parks in St. Croix, USVI

Authors

Amanda L. Bayless[1,2], Steven J. Christopher[1], Russell D. Day[3], Jennifer M. Ness[1], Colleen E. Bryan[1], C. Anna Toline[4], Cheryl M. Woodley[5]

[1]National Institute of Standards and Technology, Chemical Sciences Division, Hollings Marine Laboratory, 331 Fort Johnson Road, Charleston, SC 29412, USA

[2]The University of Charleston, SC at the College of Charleston, Grice Marine Laboratory, 205 Fort Johnson Rd., Charleston, SC 29412, USA

[3]Marine Science and Nautical Training Academy (MANTA), 520 Folly Rd, Charleston, SC 29412

[4]United States National Park Service, Region 2, South Atlantic Gulf, Stationed: Charleston, SC 29412, USA

[5]National Oceanic and Atmospheric Administration, National Ocean Service, National Centers for Coastal Ocean Science, Stressor Detection and Impacts Division, Hollings Marine Laboratory, 331 Fort Johnson Rd., Charleston, SC 29412, USA

Highlights

- Cu and Ni were above invertebrate effects ranges in SARI estuary sediment
- Coral skeleton had greater Zn and Pb at SARI reefs compared to BUIS reefs
- Coral tissue had lower $\delta^{13}C$ and $\delta^{15}N$ at SARI reefs compared to BUIS reefs

Abstract (150 words max)

Biological impairments have been documented on reefs at two national parks in St. Croix, USVI. Although several water quality parameters have been out of compliance with USVI criteria, whether these parameters or other pollutants are responsible for coral health impacts is unknown. Trace elements quantified in sediment showed four sites at SARI, which is closer than BUIS to settlements and land-derived anthropogenic outflows, had Cu mass fractions above sediment quality guidelines for invertebrate toxicity. Trace elements were also analyzed in the skeleton of threatened elkhorn coral, *Acropora palmata*, to evaluate potential exposure. Heavy metals (Pb, Zn) were significantly greater in coral skeleton at SARI than BUIS. Cu, Pb, and Zn may be impacting coral health in these parks. Potential anthropogenic sources of these metals were revealed by the coral tissue stable isotope levels ($\delta^{13}C$ and $\delta^{15}N$). These findings provide a framework for determining heavy metal impacts on these invaluable reefs.

Keywords: coral, *Acropora palmata*, trace element, stable isotope, skeleton, sediment

1. Introduction

Acropora palmata (elkhorn coral), once one of the most abundant reef building corals in the Caribbean (NMFS, 2015), has experienced population declines exceeding 80 % in the last 30 years, leading to its listing in 2006 as threatened under the U.S. Endangered Species Act (ESA) (Federal Register, 2006). Population declines have been driven by multiple global stressors including thermal-induced bleaching (Muller *et al.,* 2008), storms (Gardner *et al.,* 2005; Turgeon *et al.,* 2003), overfishing (Pittman *et al.,* 2014), and ocean acidification (Eakin *et al.,* 2010). Locally, disease (Miller *et al.,* 2009;

Patterson *et al.*, 2002; Sutherland *et al.*, 2011) and pollution (Negri *et al.*, 2002; Oliver *et al.*, 2018, 2011; Seemann *et al.*, 2013) impact populations.

Management can be effectively applied to reduce local pollutants if the sources are known, especially in state and national park jurisdiction. One park of particular concern is Salt River Bay National Historic Park and Ecological Preserve (SARI) in St. Croix, USVI (Figure 1) where water quality impairments are commonly detected including low pH, high turbidity, high fecal bacteria counts, and low dissolved oxygen (DO) (Berey, 2012; DPNR, 2018; Kendall *et al.*, 2005; Lane and Castillo II, 2017). These water quality parameters all exceeded the USVI's water quality criteria for SARI, which is Class B, established by DPNR. Detailed USVI water quality monitoring parameters for Class A, B, and C water are listed in supplementary material (Table S1). Other water quality impairments likely occur in SARI that have not been measured previously, such as heavy metals. Possible sources of copper (Cu), tin (Sn), and zinc (Zn) contamination, which have been highlighted in other studies, include marina and boat building activities, particularly anti-fouling products from watercrafts (Eklund and Eklund, 2014; Negri *et al.*, 2002). Other possible sources of metals at study sites may be derived from urban and residential areas. Heavy metals lead (Pb), Cu, and Zn can be derived from siding material for buildings and Cu from vehicle brake emissions (Davis *et al.*, 2001). These water quality impairments could be contributing to the observed decline in coral cover and coral health in St. Croix, specifically in SARI.

Human activity in St. Croix watersheds has been negatively correlated to various stony coral health metrics in adjacent water (coral condition, coral cover, colony size, colony density, coral taxa richness) (Oliver *et al.*, 2011). Furthermore, other biological impairments have been noted at various sites in SARI without links to specific contaminant sources. One example is the poor *A. palmata* reproductive output (presence of gonadal material) observed at SARI based on histological studies in 2013 and in 2017 (C.M. Woodley, personal communication). In addition to the coral histopathology, ecotoxicological studies of sediment porewater from SARI and Buck Island Reef National Monument (BUIS) in 2015 tested positive for toxicity from three of seven SARI sites (May and Woodley, 2016) in the sea urchin embryo development toxicity bioassay (ASTM, 2006), indicating that pollutants present at these sites can cause developmental aberrations in a model organism.

A lesser degree of biological impairment has been observed in BUIS, which is to the northeast of SARI (Figure 1). Only one site from BUIS had both poor *A. palmata* reproductive output (C.M. Woodley, personal communication) and tested positive in the sea urchin embryo toxicity bioassay (May and Woodley, 2016). Buck Island remains undeveloped; however, local anthropogenic pollution is a primary concern from tourism on the surrounding reefs, which attracts 40,000 to 50,000 visitors annually (Pittman *et al.*, 2014). Boating activities (*e.g.* antifouling paint compounds, fuel, grey water and raw sewage) and personal care products (*e.g.* sunscreens and insect repellents) are two main sources of pollution attributed to visitors at BUIS. BUIS is listed as Class A water and temperature has been the only parameter to exceeded water quality criteria; however, only two BUIS monitoring sites exist, which are located on the back reef, and toxicants are not being measured (DPNR, 2018).

The site-specific nature of biological impairments and the direct toxicity observed with sediment porewater suggests that poor water quality may be contributing to the observed coral decline in SARI and BUIS. Previous water quality studies have primarily focused on sites inside Salt River Bay. The extent of coral exposure to pollutants is poorly understood since the reefs within the SARI park boundaries are located near the mouth and to the north of Salt River Bay. Furthermore, analyses have not been performed at these sites for either heavy metal pollutants or basic water quality parameter impairments focusing on coral exposure. To accomplish this, a trace element analysis in both sediment and coral skeleton and a stable isotope analysis in coral tissue were conducted on samples from SARI and BUIS.

Elemental analysis of reef sediment has been widely used to assess site contamination (Acevedo-Figueroa *et al.,* 2006; Bernard, 1995; Gonzalez *et al.,* 1999; Guzmán and Jiménez, 1992; Jaffé *et al.,* 2003; Long *et al.,* 1995; Rajkumar and Persad, 1994; Sbriz *et al.,* 1998) and is specifically used to interpret or calculate metal bioavailability in order to quantify potential toxicity of these chemicals to marine organisms (Acevedo-Figueroa *et al.,* 2006; Ali *et al.,* 2011; Chiappetta *et al.,* 2016; Fujita *et al.,* 2013; Nobi *et al.,* 2010; Ratheesh Kumar *et al.,* 2010). Sediment is favored over water column analysis for these contaminants because over 90 % of heavy metals in the aquatic environment are bound to sediment (Calmano *et al.,* 1993). Thus, analyzing sediment loads is advantageous for identifying long-term reservoirs and providing evidence for potential sources from contaminant "hot spots".

Coral incorporate elements from both the sediment and water column into skeleton and soft tissues during growth and metabolism. Coral tissue analysis provides insight on real-time toxic metal body-burdens and direct evidence of biological availability, while the coral skeleton can be used to interpret water quality parameters that affect bioavailability along with a long-term record of anthropogenic pollution and exposure (Al-Rousan *et al.,* 2012; Anu *et al.,* 2007; Druffel, 1997; El-Sorogy *et al.,* 2013; Krishna Kumar *et al.,* 2010; Prouty *et al.,* 2008; Ramos *et al.,* 2004; Al-Rousan *et al.,* 2007). Corals secrete calcium carbonate ($CaCO_3$) to form a skeleton using calcium (Ca) ions from the seawater. Water soluble elements (metals and non-metals) other than Ca are assimilated into the skeleton via ion exchange between Ca and the respective element during skeleton formation (Ramos *et al.,* 2004; Sinclair *et al.,* 1998). Metal assimilation into skeleton also occurs by ingestion of zooplankton and particulates (Howard and Brown, 1984) and by adsorption of organic matter and particulates that become trapped in the aragonite upon additional skeletal growth (Brown *et al.,* 1991).

The metals in the skeleton provide a record of pollution by showing clear changes in biomineralization from pre- to post-industrialization and changes in skeletal concentrations that mirror the expansion of coastal development (Al-Rousan *et al.,* 2007). Trace elements present in coral skeleton also are proxies of physico-chemical water quality parameters (*e.g.* salinity, temperature, pH). Altered water quality parameters, such as excess nutrients, freshwater input, sedimentation, turbidity, and differences in pH and temperature, can be detected via elemental proxies that respond to the changes in these parameters. For example, strontium (Sr) to Ca ratios (Sr/Ca) along with lithium (Li) to magnesium (Mg) ratios (Li/Mg) in coral skeleton correlate well with sea surface temperature (SST), so these skeletal ratios are used in the field of paleoclimatology to reconstruct historic SST (Fowell *et al.,* 2016). Coral skeletons can provide a record of freshwater inputs into the system by examining barium-calcium ratios (Ba/Ca) with greater Ba/Ca values indicating increased freshwater input (Macdonald and Crook, 2010). Skeletal boron-calcium ratios (B/Ca) have also been shown to change with the pH of the surrounding seawater (DeCarlo *et al.,* 2018; Fowell *et al.,* 2018; Sanyal *et al.,* 2000).

Stable isotopes can be used as proxies to further understand the type of chemical exposures affecting coral reefs. The delta (δ) values (the amount ratios of $^{13}C/^{12}C$ and $^{15}N/^{14}N$ isotope relative to scale standards with known isotopic composition) of carbon ($\delta^{13}C$) and nitrogen ($\delta^{15}N$) stable isotopes can provide information about chemical, physical, and biological processes. The interpretation of delta values in a marine organism can be very complex, because it not only involves examining the inputs, outputs, and internal oceanic cycling (Sigman *et al.,* 2009), but it also involves examining cycling within the organism and includes food web contributions. The $\delta^{13}C$ reveals information about the carbon sources, whether they are terrestrial or oceanic, and how they have been impacted by the carbon cycle. For example, carbon that is used to form an algal cell, such as those residing in coral, is initially derived from dissolved inorganic carbon, which has a delta value of 0‰ in seawater (Ohkouchi *et al.,* 2015). As the inorganic carbon is assimilated by the algae, fractionation occurs because the algae discriminate against

the heavy isotope based on utilization (Titlyanov *et al.*, 2008). Similarly, source information can be garnered from δ^{15}N. Nitrogen stable isotopes are typically used to determine terrestrial input into an environment, such as fertilizer runoff or wastewater input, because of the distinct δ^{15}N signatures for terrestrial versus oceanic derived nitrogen (Peterson and Fry, 1987). Nitrogen stable isotopes are also used to determine trophic level (Nahon *et al.*, 2013). Generally, greater δ^{15}N (ie. decreased nitrogen availability) is indicative of greater primary productivity, like that which would be observed in the coral's algal symbionts (Brenner *et al.*, 1999). In contrast, heterotrophic feeding results in a lower δ^{15}N because biological processes preferentially assimilate ^{14}N (Hoegh-Guldberg *et al.*, 2004). Therefore, isotopic signatures of carbon and nitrogen in the coral tissue can be used to determine the coral's primary food source (autotrophic or heterotrophic) and the coral's exposure to anthropogenic inputs, such as wastewater and fertilizer. This in combination with the trace element proxies in the coral skeleton alludes to biological exposure and the nature of the primary exposure source.

The aim of this study was to determine *A. palmata*'s exposure to trace element pollutants and other water quality stressors with four types of analyses: 1) trace elements in the sediment were measured to compare the degree of contamination between sites; 2) sediment grain size distribution was analyzed to aid in interpreting trace element mass fraction differences and bioavailability; 3) trace elements in coral skeleton samples were quantified to provide a record of exposure; and 4) δ^{13}C and δ^{15}N stable isotope analyses were performed on the coral tissue to investigate *A. palmata*'s exposure to terrestrial versus oceanic sources of carbon and nitrogen.

2. METHODS

2.1 Sampling

Coral biopsies were collected from seven sites (≤ 3 m water depth) in St. Croix, USVI (July 25-27, 2017; Figure 1) where there were remaining *A. palmata* colonies with less than 50 % colony tissue mortality (NPS Research Permit No. SARI-2017-SCI-0007, NPS Research Permit No. BUIS-2017-SCI-0009, and DPNR CZM Research Permit CZM 17012X). Ten *A. palmata* colonies of reproductively mature size (> 0.19 m^2) were sampled at each site with one biopsy taken from each colony, except at site BUIS 4 (only four colonies were present). Biopsies (approximately 1.5 cm^2) were collected by SCUBA divers wearing clean nitrile gloves and using a stainless steel hammer and chisel. Chisels were pre-cleaned with isopropanol and Type I high-purity deionized water (resistivity = 18 MΩ-cm; TOC < 5 ppb). New gloves and a clean chisel were used for each colony to prevent specimen cross-contamination. Location of the biopsies on the colony was on the upward facing surface of the branches, at least 2 cm away from the growing edges, and on a sturdy portion of the branch that could withstand chiseling without breakage. Coral biopsies were placed into plastic Whirl-Pak bags underwater. Immediately on reaching the surface, excess seawater was removed, and biopsies were transferred to individual perfluoroalkoxy (PFA) jars (Savillex, Eden Prairie, MN) and snap-frozen in a liquid nitrogen (LN_2) vapor shipper (≤ -150º C).

Sediment (n = 3 per site) was collected at the time of coral sampling from 15 sites (n = 45 sediment samples) within a 2 m by 2 m area at each location (Figure 1). Sediment was collected from all sites where coral was sampled (except BUIS 6), and additional samples were taken within the SARI estuary due to the park's significance and the proximity to potential pollution sources. Sampling sites within SARI also had < 3 m water depth. The top layer of sediment, approximately 3 cm, was collected by filling acid washed 50 mL polypropylene tubes. The tubes immediately were placed into a cooler and then frozen in the interim at -20 °C at the end of each sampling day. Coral and sediment samples were transferred to a -80 °C freezer on return to the Charleston laboratory until analysis. Additional sampling

information can be found in supplementary material: GPS coordinates (Table S2), coral percent tissue mortality and colony size (Table S3), and sediment images (Figure S1). Water temperature, salinity, pH, DO, nutrients, Secchi depth, total suspended solids, turbidity, and enterococcus were measured by other agencies at various sites around SARI and BUIS in 2017. This water quality data was obtained from the Water Quality Portal (https://www.waterqualitydata.us/portal/) and compiled in supplementary material (Table S4).

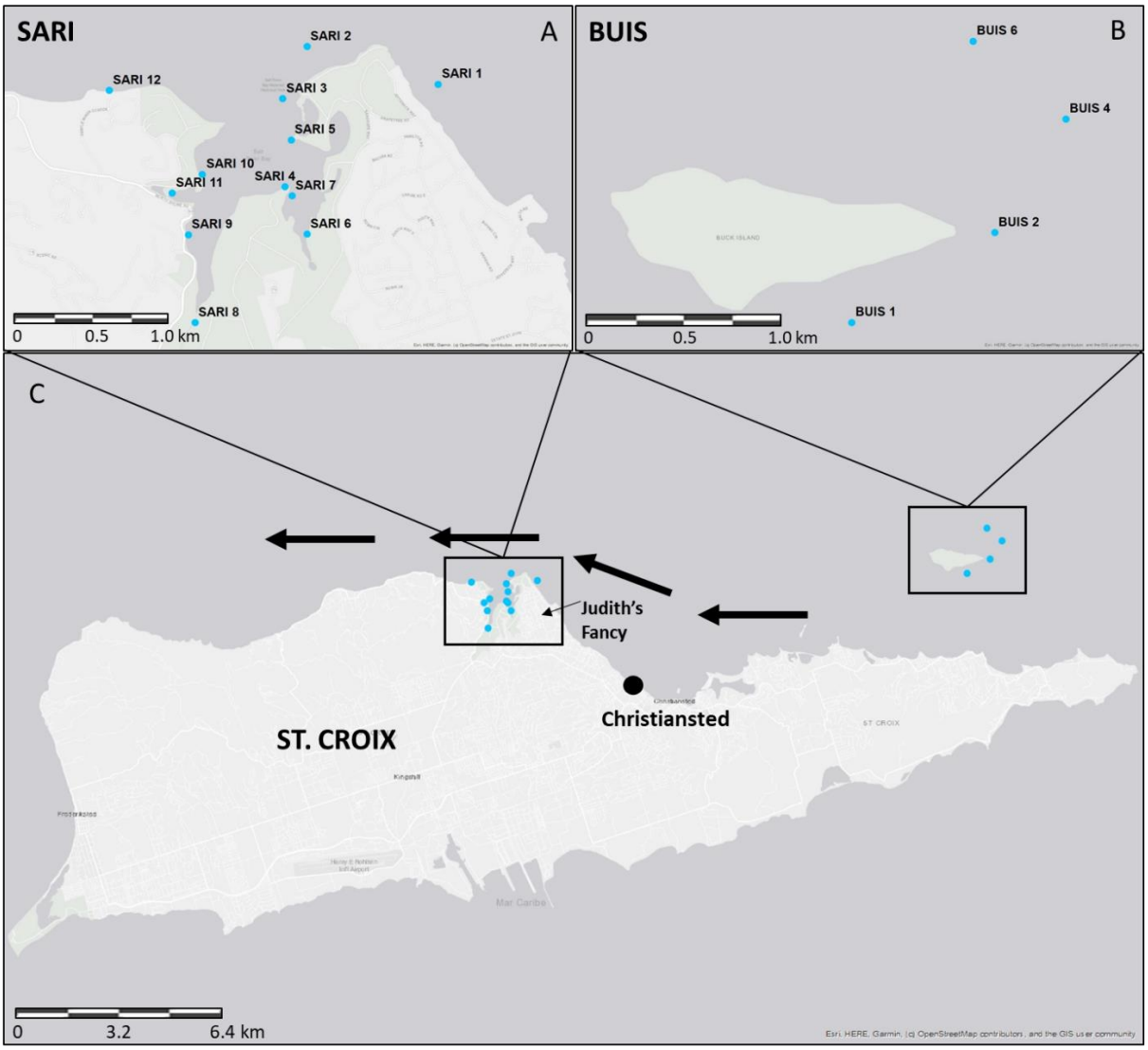

Figure 1. *Acropora palmata* and sediment sampling sites at Salt River Bay National Historic Park and Ecological Preserve (SARI) and at Buck Island Reef National Monument (BUIS). Sediment and coral were sampled both at SARI (A) and at BUIS (B) in St. Croix, USVI (C). Sediment was sampled at all sites except BUIS 6 (n = 15 sites). Coral was sampled at SARI 1 to 3 and at all BUIS sites (n = 7 sites). The black arrows represent the direction of the longshore current, and the circle depicts the location of a major Waste Management Authority pump station.

2.2 Sample Preparation

The sediment was lyophilized in a bulk drying lyophilizer (VirTis Genesis 25XL) for 96 h with the shelf at room temperature and then coarsely sieved at 1 mm with a #18 3-inch stainless steel sieve (Cole-Parmer, Vernon Hills, IL). Sediment digestion was performed using a modified method of Durand *et al.* (2016). All samples and standards were prepared gravimetrically. Sediment digestion was done in polytetraflouroethylene (PTFE) microwave vessels with approximately 200 mg of sediment; 200 mg of internal standard solution containing NIST SRM 3124a Indium (In) (Lot No. 110516) and NIST SRM 3167a Yttrium (Y) (Lot No. 120314); and 4 mL of high purity grade hydrochloric acid (HCl) (Fisher Scientific Optima). First, the vessels were placed in a hot block at 150 °C for 2 h to assist in dissolving carbonates and to evolve carbon dioxide (CO_2). Next, 2 mL of hydrofluoric acid (HF) and 10 mL of nitric acid (HNO_3), both high purity grade (Fisher Scientific Optima), were added to the samples followed by microwave digestion in a MARS 5 microwave system (CEM, Matthews, NC). The microwave digestion method consisted of a 20 min ramp to 210 °C and the samples were held at 210 °C for 30 min. Samples were then placed back into the 150 °C hot block to evaporate the HF. An additional 4 mL of HNO_3 was added to each sample and diluted with high-purity deionized water to 2 % HNO_3 for elemental analysis by inductively coupled plasma mass spectrometry (ICP-MS).

Coral biopsies were ground into a homogenous fine powder using cryogenic grinding in a stainless steel CryoMill (Retsch, Hahn, Germany). Subsamples (≈ 150 mg) of the frozen tissue-skeleton homogenate were oxidized at room temperature using 5.65 % to 6.0 % sodium hypochlorite (NaClO) (Fisher Scientific Optima) to digest and remove coral soft tissue. The samples were mixed on a Roto-Shake Genie (Model No. SI-1100, Scientific Industries, Inc.) over 48 h at room temperature. The tissue and NaClO supernatant was removed from the vials and 4 mL of high-purity deionized water were added to rinse the skeleton. Vials were vortexed, and when the skeleton was settled (≈ 5 min), the top 4 mL of water was removed using a plastic pipette. The ground coral skeleton was rinsed 3 times using this process. After rinsing, the coral skeleton powder was frozen at -80 °C and lyophilized for 48 h. Samples were dissolved in 50 mL of 0.5 mol/L HNO_3. An aliquot was taken from each sample and diluted with high-purity deionized water approximately 6,000 fold in order to obtain Ca mass fractions within operating range of the ICP-MS.

2.3 Sediment and Coral Skeleton Elemental Analysis

Multi-element analysis of sediment and coral skeleton was carried out on an Agilent 8800 Triple Quadrupole (QQQ) ICP-MS system (Agilent, Santa Clara, CA). All elements were measured using either no gas, helium (He), or oxygen (O_2) collision/reaction gas to reduce interferences. The suite of elements analyzed in coral skeleton and sediment varied slightly, but 26 elements were measured in each sample type. Calibration standards were gravimetrically prepared using NIST SRM 1643f Trace Elements in Water for the sediment calibration curve. A custom multi-element standard solution was prepared to mimic a coral matrix using NIST SRM 3100 series single element standard solutions and single element standards from High Purity Standards Inc. (Charleston, SC) for the coral calibration curve.

The reported trace element mass fractions (mg/kg) in the analytical samples were calculated based on linear regression calibration using internal standards, multiplying by the dilution factor, and correcting for moisture. NIST SRM 3124a Indium (In) Standard Solution (Lot No. 110516) was used as the internal standard for elements measured in no gas and helium gas modes, and SRM 3167a Yttrium (Y) Standard Solution (Lot No. 120314) was used as the internal standard for elements measured in oxygen mass shift mode. The controls used for the sediment analyses were NIST SRM 2702 Inorganics in Marine Sediment and NIST SRM 1944 New York/New Jersey Waterway Sediment. The control used for

coral skeleton analyses was National Institute of Advanced Industrial Science and Technology (AIST) Certified Geochemical Reference Material JCp-1 Coral, which was prepared and distributed by the Geological Survey of Japan (note: no longer available). JCp-1 was processed alongside the *A. palmata* skeleton experimental samples using the same methods. The assigned mass fraction values for the NIST SRMs and JCp-1 (https://gbank.gsj.jp/geostandards/Certificate/PDF/eJCp1.pdf) are comprised of certified and non-certified data. Comparing control results to the non-certified data assist with evaluating the method for additional elements, but these comparisons do not account for any method biases in either the measured or assigned values. The evaluation of the measured values to the assigned values for these controls are shown in supplementary material (Figures S2-S4) and the values obtained for JCp-1 are listed in Table S5.

Total mercury (Hg) was only measured in sediment by direct combustion atomic absorption spectrophotometry (AAS) using a DMA-80 (Milestone Scientific, Shelton, CT). Approximately 100 mg of each sediment sample was weighed into nickel sample boats, thermally decomposed, catalytically reduced to Hg^0, and trapped on a gold amalgamation trap. The Hg was then thermally desorbed and the Hg atomic absorption measured at 254 nm. Mercury mass fractions were determined with external calibration curves (peak area versus ng Hg) prepared with NIST SRM 3133 Mercury Standard Solution (Lot No. 160921). A second-order line of fit was applied to the calibration curves to account for the asymptotic curve produced by the instrument fundamental to Beer-Lambert's Law. Sediment sample Hg mass fractions were then calculated using the second order fit coefficients and peak areas to solve the quadratic equation. SRM 1566b Oyster Tissue was used as the control material for Hg analysis quality assurance.

2.4 Sediment Grain Size Analysis

A grain size analysis was performed on the sieved sediment samples (≤ 1 mm) using a Malvern Mastersizer 3000 laser diffraction particle size analyzer (Malvern Instruments Inc., Westborough MA) fitted with a Hydro EV wet dispersion unit and high-purity deionized water was used as the dispersant. The refractive index was 1.33 for the water dispersant and 1.5 for the sediment. Sediment was added to 1.0 L of the water dispersant until the obscuration reached approximately 10 %. A background measurement of the dispersant was made prior to adding the sample, and it was subtracted from the final measurement. Ten sample measurements, 10 s each, were made by the instrument to obtain an average distribution. The particle size measurement is based on the equivalent spherical diameter and is reported as the median of the average volume distribution for each site. The sediment type (*e.g.* clay, silt, sand) at each site was determined according to classification sizes by USDA (1987). The average volume particle size distribution from the three sediment replicates was converted to percentages for each size classification using the mass of the whole sample including the > 1 mm fraction, which was sieved off prior to the particle size analysis. NIST SRM 1944 and Malvern Panalytical Quality Audit Standard glass beads were used as controls. All measurements were assessed on their compliance with the International Organization for Standardization's (ISO) definition of reproducible data (ISO, 2020). The value used for assessment was the ISO relative standard deviation (RSD) for the Dx90, Dx50, and Dx10, which is the maximum particle volume below which 90 %, 50 % and 10 % of the sample volume exists, respectively. The ISO RSD limits are < 5 % RSD for Dx90 and Dx10, and < 3 % for Dx50.

2.5 Stable Isotope Analysis

Acropora palmata tissue was analyzed by the Skidaway Institute Scientific Stable Isotope Laboratory (Savannah, GA) for total C (%), N (%), $^{13}C/^{12}C$ and $^{15}N/^{14}N$ using a Thermo Flash elemental analyzer coupled to a ThermoFisher Delta V plus isotope ratio mass spectrometer (Thermo Fisher

Scientific, Waltham, MA) and methods from Fry *et al.* (1992). Ten samples were analyzed from each site, except BUIS 4, where only three biopsies had sufficient tissue for stable isotope analysis. Measurements for $\delta^{15}N$ were made on the whole sample (skeleton, tissue, and zooxanthellae), but for $\delta^{13}C$ only organic carbon was analyzed. Inorganic carbonate can confound the organic $\delta^{13}C$ measurements, so inorganic carbon was removed via acid fumigation using HCl (Hedges and Stern, 1984). In contrast, acid fumigation can change the ^{15}N abundance and was not used for $\delta^{15}N$ analysis (Harris *et al.*, 2001). Isotopic values were calibrated using chitin internal standards (MilleporeSigma, St. Louis, MO). Samples were calibrated based on the international standard: NIST Reference Material 8573 L-glutamic Acid USGS40. This reference material was used to measure relative differences in the coral C and N isotope ratios compared to the Vienna Pee Dee Belemnite (VPDB) standard for C and the atmospheric air standard for N. The ratios that have been established for these materials as the $\delta^{13}C$ and $\delta^{15}N$ value of zero are 0.01123720 ($^{13}C/^{12}C$) and 0.0 ($^{15}N/^{14}N$).

2.6 Data Processing and Statistical Analysis

Instrument blanks, acid washed 50 mL polypropylene tubes containing 2 % HNO_3, were used for measuring the QQQ-ICP-MS instrument background and were subtracted from all analytical samples and procedural blanks to account for any sample contamination or sample carry over from the instrument. The most recently measured instrument background in the sample queue was used for subsequent samples. Procedural blanks were clean empty microwave vessels that underwent all sediment digestion steps. Procedural blanks showing contamination of any elements after the instrument background was subtracted were then subtracted from the analytical sample mass fraction. Procedural blanks for Hg analysis were empty nickel sample boats that underwent the same AAS methods as sediment samples and the mean blank mass fraction was subtracted from analytical samples.

All mass fraction data are reported on a dry mass basis in units of µg/g, ng/g, or % depending on the analyte and magnitude. Element mass fractions in the sediment and median grain size were log transformed for normality for all analyses. Elements in the sediment were compared by sediment type: SARI No Reef (SARI sediment not co-located with any coral: *SARI 4-11*), SARI Reef (SARI sediment co-located with *A. palmata* reefs: *SARI 1-3, 12*), and BUIS Reef (BUIS sediment co-located with *A. palmata* reefs: *BUIS 1, 2, 4*). Elements grouped by sediment type were analyzed using either Tukey's HSD test (parametric) or Dunn's test (non-parametric). Elements in the sediment were also analyzed by site using either Tukey's HSD test or Dunn's test. Median grain size was analyzed between sites using Tukey's HSD test.

All elements in the coral skeleton were compared using the trace element (X) to Ca mass fraction ratio (X/Ca). The Ca acts as a sample matrix internal standard and was used to normalize data between sample runs. All trace element to Ca mass fraction ratios were examined for differences between sites using Tukey's HSD test or using Dunn's test with Bonferroni correction. Trace element mass fraction ratios in the skeleton also were compared between SARI and BUIS using either a t-test or a non-parametric Kruskal-Wallis test. A two sample t-test was used to compare coral $\delta^{13}C$ between SARI and BUIS and to compare coral $\delta^{15}N$ between SARI and BUIS. Tukey's HSD pairwise comparison was used to detect differences among sites within SARI and within BUIS.

3. RESULTS AND DISCUSSION

3.1 Sediment Trace Element Analysis

Salt River Bay and Buck Island contain similar geologic composition with limestone, volcaniclastics, mudstone, and sandstone (Alminas *et al.*, 1994; Gill *et al.*, 2004; KellerLynn, 2011;

Kendall *et al.*, 2005). St. Croix and the rest of the US. Virgin Islands also have a unique metal mineralization and contain naturally derived Au, Ag, Te, Sn, Pb, Cu, Zn, Ni, Cr, Sb, As, Bi, Mo, Cl, and Ba (Alminas *et al.*, 1994). These elements should be constituents of the terrigenous sediments found in St. Croix. When examining element differences in the sediment by sediment type (SARI estuary sediment, SARI reef sediment, and BUIS reef sediment), 18 elements (Li, Be, Na, Al, K, V, Cr, Mn, Fe, Ni, Cu, Zn, Rb, Mo, Ba, Hg, Tl, Pb) were found at significantly greater mass fractions in SARI estuary sediment than in SARI reef and BUIS reef sediment ($p < 0.05$). For the SARI and BUIS reef sediments, mass fractions of Mg, K, V, Mn, Cu, Zn, As, Rb, Ba, Hg, and Pb were all significantly greater in the SARI reef sediment than BUIS, while only Sr was significantly greater in the BUIS reef sediment than SARI ($p < 0.05$). The sediment composition differences that are derived from natural inputs are a result of different types of erosion since the geologic composition is similar at SARI and BUIS. Sediments around Buck Island and outside of Salt River Bay are primarily carbonate from reef erosion, while the sediments within Salt River Bay are mostly terrigenous input. There is occasional transport of the terrigenous material from within Salt River Bay to the nearby reefs, particularly during storms, which is the likely cause of a greater Sr mass fraction at BUIS reef sites compared to the greater metal mass fractions observed at SARI reef sites (Hubbard, 1992). Sediment mass fraction values for all analytes are shown in Table 1 as summary statistics for SARI estuary, SARI reef, and BUIS reef. The sediment mass fractions found at each site are listed in supplementary material (Table S6, Table S7).

The elevated mass fractions of Cu and Ni suggest anthropogenic sources are also contributing to the observed sediment trace element composition. Copper was of particular concern because it was above effects range low (ERL) concentrations, which are estimated to rarely cause adverse effects (< 10 % frequency) in benthic organisms (Long and Morgan, 1991, Long *et al.*, 1995). Copper exceeded the ERL at four estuary sites (SARI 6, SARI 8, SARI 9 and SARI 11; Figure 2), and while coral was not used to develop these sediment quality guidelines, Cu can be very toxic to coral. Laboratory studies using copper chloride decreased the motility of *Goniastrea aspera* coral larvae at concentrations as low as 16 µg/L Cu (Reichelt-Brushett and Harrison, 2004) and inhibited fertilization of *A. millepora* coral by 50 % with 17.4 µg/L Cu (Negri and Heyward, 2001). Copper in the form of copper sulfate ($CuSO_4$) also reduces fertilization by 10 % relative to the control of *A. aspera* gametes at 5.8 µg/L Cu (Gissi *et al.*, 2017) and is known to inhibit photosynthetic efficiency in coral algal symbionts at 50 µmol/L Cu (Kuzminov *et al.*, 2013). Copper has been found in sediments near boats (Smith *et al.*, 2003), likely derived from the cuprous oxide in boat antifouling paint. Contaminated sediment near a sunken boat contained 72 µg/g Cu, along with other antifouling compounds from the boat paint, and exposure to the sediment inhibited *A. microphthalma* coral larvae settlement and metamorphosis *(Negri et al.*, 2002). Thus, Cu contaminated sediment (up to 82.2 µg/g) in Salt River Bay may be similarly toxic to coral and be associated with sunken boats as well as marina, boat building, and other boat related activities.

Nickel was above the ERL at SARI 8 (24.6 µg/g ± 1.83 µg/g SE) and may be of concern for coral as documented in laboratory studies. Reproductive output in copepods was shown to be significantly reduced with Ni concentrations as low as 10 µg/L (Mohammed *et al.*, 2010). Fertilization of gametes was also inhibited in *Acropora aspera* and *Acropora digitifera* with exposure to Ni (NOEC < 280 µg/L and EC_{10} of 2000 µg/L, respectively) (Gissi *et al.*, 2017). Arsenic was also above the ERL at SARI 6, but the result should be interpreted with caution. The measured values for As in the controls NIST SRM 1944 and NIST SRM 2702 were approximately 20 % greater than the certified values even after correction for the possible $ArCl^+$ interference. The greater measured values for As in the controls likely resulted from ICP source differential ionization effects that enhanced ionization of As in samples containing residual carbon relative to the calibration standards (Larsen and Stürup, 1994), and this effect would translate to the study samples. Other analyte concentrations found in the sediment that were not above the ERL may

still be toxic to coral. Sediment Quality Guidelines have not been developed for all analytes, and values were not established based on coral's toxicity response since coral exposure data was unavailable.

Table 1. Summary statistics for trace elements in the SARI estuary, SARI reef, and BUIS reef sediment samples. All mass fraction values are in µg/g, dry mass fraction. Sediment Quality Guidelines (SQG) are from Long *et al.* (1995) that compiled various toxicity studies. Toxicity ranges of select elements were calculated based on sediment mass fractions that caused adverse effects in benthic organisms in the lower 10th percentile (effects range low = ERL) or in the 50th percentile (ERM = effects range median). Element values in bold are above the ERL.

	SARI Estuary					**SARI Reef**					**BUIS Reef**					**SQG**	
Element	Mean	±SE	Med	Min	Max	Mean	±SE	Med	Min	Max	Mean	±SE	Med	Min	Max	ERL	ERM
Li	11.6	3.54	8.46	3.31	30.8	1.74	0.19	1.57	1.51	2.32	0.77	0.05	0.79	0.68	0.84	-	-
Be	0.24	0.07	0.18	0.02	0.57	0.04	0.00	0.04	0.03	0.05	0.01	< 0.01	0.01	< 0.01	0.01	-	-
B	27.3	9.62	13.4	6.20	75.4	32.7	1.91	31.2	30.1	38.3	40.3	0.33	40.4	39.7	40.8	-	-
Na	24837	5996	17858	10365	56817	7411	430	7548	6240	8311	8027	408	8006	7330	8744	-	-
Mg	14212	1126	14687	9881	18965	15490	688	15255	14093	17356	10610	1267	11502	8110	12218	-	-
Al	29648	7582	26596	6903	61251	3906	737	4005	2079	5534	75.5	25.5	82.9	28.1	116	-	-
K	4901	1242	3946	1319	10584	837	127	874	513	1090	316	46.7	285	255	408	-	-
V	51.9	14.2	44.2	11.5	115	6.09	0.41	6.14	5.13	6.94	0.40	0.08	0.37	0.27	0.55	-	-
Cr	20.2	4.33	19.2	4.94	34.6	4.26	0.47	4.04	3.45	5.49	2.72	0.25	2.66	2.32	3.17	81.0	370
Fe	19607	5263	18825	3751	42270	1935	197	2083	1367	2209	56.1	14.3	62.9	28.6	76.8	-	-
Mn	327	79.8	279	126	789	95.5	13.8	87.5	73.8	133	11.7	3.11	11.8	6.23	17.0	-	-
Ni	11.8	2.94	9.41	3.08	**24.6**	1.46	0.07	1.49	1.27	1.61	0.77	0.09	0.71	0.65	0.96	20.9	51.6
Cu	33.3	10.6	28.3	3.24	**82.2**	1.56	0.15	1.58	1.16	1.90	0.44	0.18	0.27	0.24	0.81	34.0	270
Zn	59.5	15.5	60.0	14.3	147	5.20	0.80	5.47	3.28	6.58	0.82	0.15	0.77	0.59	1.09	150	410
As	3.82	1.18	2.39	1.03	**11.1**	2.45	0.30	2.26	1.99	3.27	0.82	0.10	0.84	0.63	0.98	8.20	70.0
Se	1.07	0.38	0.74	0.32	3.56	0.09	0.01	0.09	0.07	0.12	0.07	0.00	0.07	0.06	0.07	-	-
Rb	10.4	2.96	7.77	2.28	24.5	1.20	0.21	1.25	0.73	1.57	0.12	0.03	0.13	0.08	0.16	-	-
Sr	2866	569	3332	187	4728	3595	149	3607	3222	3945	5407	196	5287	5144	5790	-	-
Mo	< 0.01	< 0.01	< 0.01	< 0.01	< 0.01	0.15	0.02	0.14	0.11	0.21	0.15	0.03	0.17	0.10	0.20	-	-
Ag	0.05	0.02	0.04	0.00	0.11	0.02	< 0.01	0.02	0.01	0.02	0.01	< 0.01	0.01	0.01	0.02	1.00	3.70
Cd	0.07	0.02	0.06	0.02	0.15	0.03	< 0.01	0.03	0.03	0.04	0.01	< 0.01	0.01	0.01	0.01	1.20	9.60
Sb	0.21	0.04	0.18	0.11	0.36	0.09	0.02	0.09	0.03	0.12	0.02	< 0.01	0.02	0.01	0.02	-	-
Te	0.06	0.02	0.04	0.01	0.18	0.01	< 0.01	0.01	< 0.01	0.01	< 0.01	< 0.01	< 0.01	< 0.01	< 0.01	-	-
Ba	119	35.8	94.0	29.4	337	29.2	7.04	29.5	11.8	45.9	8.58	0.58	8.60	7.56	9.57	-	-
Tl	0.13	0.03	0.11	0.02	0.27	0.03	0.01	0.02	0.02	0.05	0.01	< 0.01	0.01	< 0.01	0.01	-	-
Pb	6.13	2.31	3.80	1.18	20.2	1.06	0.16	0.94	0.84	1.53	0.36	0.08	0.32	0.23	0.52	46.7	218
Hg	0.02	0.01	0.02	< 0.01	0.06	< 0.01	< 0.01	< 0.01	< 0.01	0.01	< 0.01	< 0.01	< 0.01	< 0.01	< 0.01	0.15	0.71

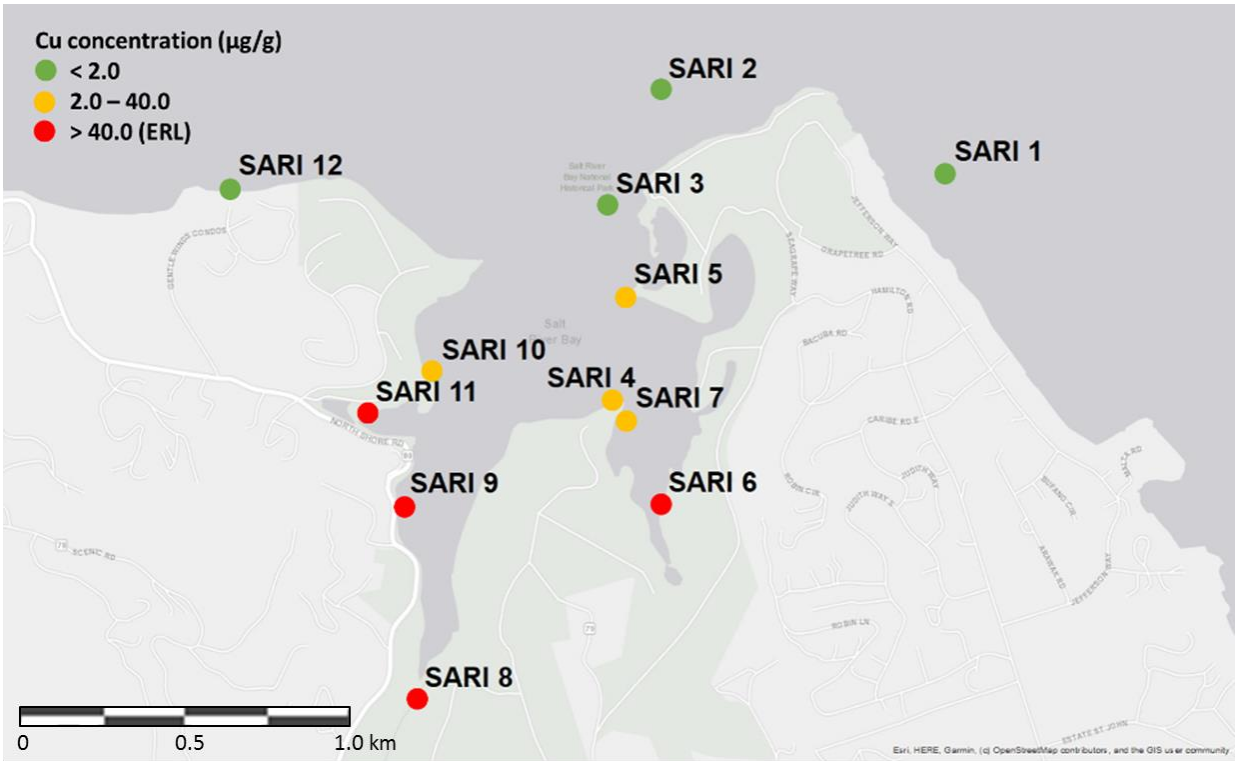

Figure 2. Sediment Cu mass fractions (µg/g) in SARI. SARI 6, 8, 9 and 11 had concentrations above the ERL (> 40.0 µg/g) and are marked with red circles. All sites had < 3 m water depth.

The total chemical mass fractions from the grab sediment samples provided baseline data that are useful for interpreting trace element loads in SARI and BUIS, which were comparable to other Caribbean studies. The element mass fractions in the St. Croix sediments were similar to sediment analyzed in Puerto Rico (Whitall *et al.,* 2014) and St. John, USVI (Whitall *et al.,* 2015). Another study in the St. Thomas East End Reserves, USVI indicated a few sites with mass fractions consistently greater than those obtained in this study (Pait *et al.,* 2016). The aforementioned sediment studies exhibited good quality assurance and quality control with use of certified reference materials, and detailed analytical methods were referenced. While these inter-study comparisons are helpful for identifying contaminated sediment, further sediment analysis, such as sequential leaching (Tessier *et al.,* 1979), or detailed water quality could reveal more information about bioavailability and toxicity. A decrease in pH (below 7.0) and an increase in temperature (at 30-35 °C) decrease the adsorption and precipitation of heavy metals, which makes them more soluble and ultimately bioavailable (Belzile *et al.*, 2004; Li *et al.*, 2013; Martín-Torre *et al.*, 2015). This suggests that the pH water quality impairments at SARI and the elevated SST at BUIS are influencing the toxicity potential of heavy metals. Furthermore, elevated SST and low pH alone can negatively influence coral health, and when coupled with toxic concentrations of heavy metals, these water quality impairments may cause confounding effects. One example of confounding toxicity was shown by Negri and Hoogenboom, (2011). As temperature increases, the coral larvae metamorphosis EC_{50} for Cu also decreases. Thus, these contaminants can become more bioavailable and more toxic as the environmental conditions change.

3.2 Sediment Grain Size Analysis

Median grain size at SARI was significantly different from BUIS; however, grain size also significantly varied among sites within each park, among reef sites, and among estuary sites (Figure 3). Images of a representative sediment sample from each site are shown in Figure S1 demonstrating the

differences in sediment composition. All samples were classified as mostly sand or very coarse sand and gravel based on the average volume particle size distribution, but SARI 8 contained 35 % silt (Table 2). Some of the sediment replicates passed the ISO RSD criteria (ISO, 2020), but most samples did not pass due to the natural variability of sediment which creates a non-uniform distribution. The RSDs were as follows: Dx10 < 15.5 % RSD; Dx50 < 11 % RSD with an exception for 1 replicate from SARI 7 (27.9 % RSD); Dx90 < 23 % RSD. The laser diffraction method for particle size analysis has been shown to provide comparable results to a sedimentation method (Fisher *et al.*, 2017) and was relatively quick and efficient for determining sediment grain size.

Silt and very fine sand are associated with the greatest concentrations of adsorbed trace elements due to their greater surface area to volume ratio than larger sediment particles (Horowitz and Elrick, 1987). SARI 8 is the most interior site of Salt River Bay and has the greatest potential to act as a reservoir of contaminants with the small grain size. Finer sediment grains are also more susceptible to resuspension in the water column and slower settling, creating turbidity and a greater chance for sedimentation on coral. Turbidity can attenuate light available to the symbiotic algae (dinoflagellates) of stony corals, reducing autotrophy and resulting in coral starvation and increased hypoxia (Jones *et al.*, 2016; Rogers, 1979). The mechanisms of sedimentation damage on coral are less clear due to inconsistent methodology, but various authors have speculated that this damage could induce both chemical and physical effects (Jones *et al.*, 2016; Vargas-Ángel *et al.*, 2007; Weber *et al.*, 2012). Sediment enriched in organic matter was shown to increase microbial activity leading to degradation of coral tissue in mesocosm studies (Weber *et al.*, 2012). Other chemical effects may include increased contaminant and nutrient availability via desorption from sediments (Jones *et al.*, 2016). Sediment accumulation on corals can also cause increased mucus production, increased self-cleaning, and reduced feeding, all of which could reduce energy allocated to growth and reproduction (Jones *et al.*, 2016). The stressors associated with the increased turbidity of small grain size combined with the contaminant exposure could produce confounding negative effects on the coral.

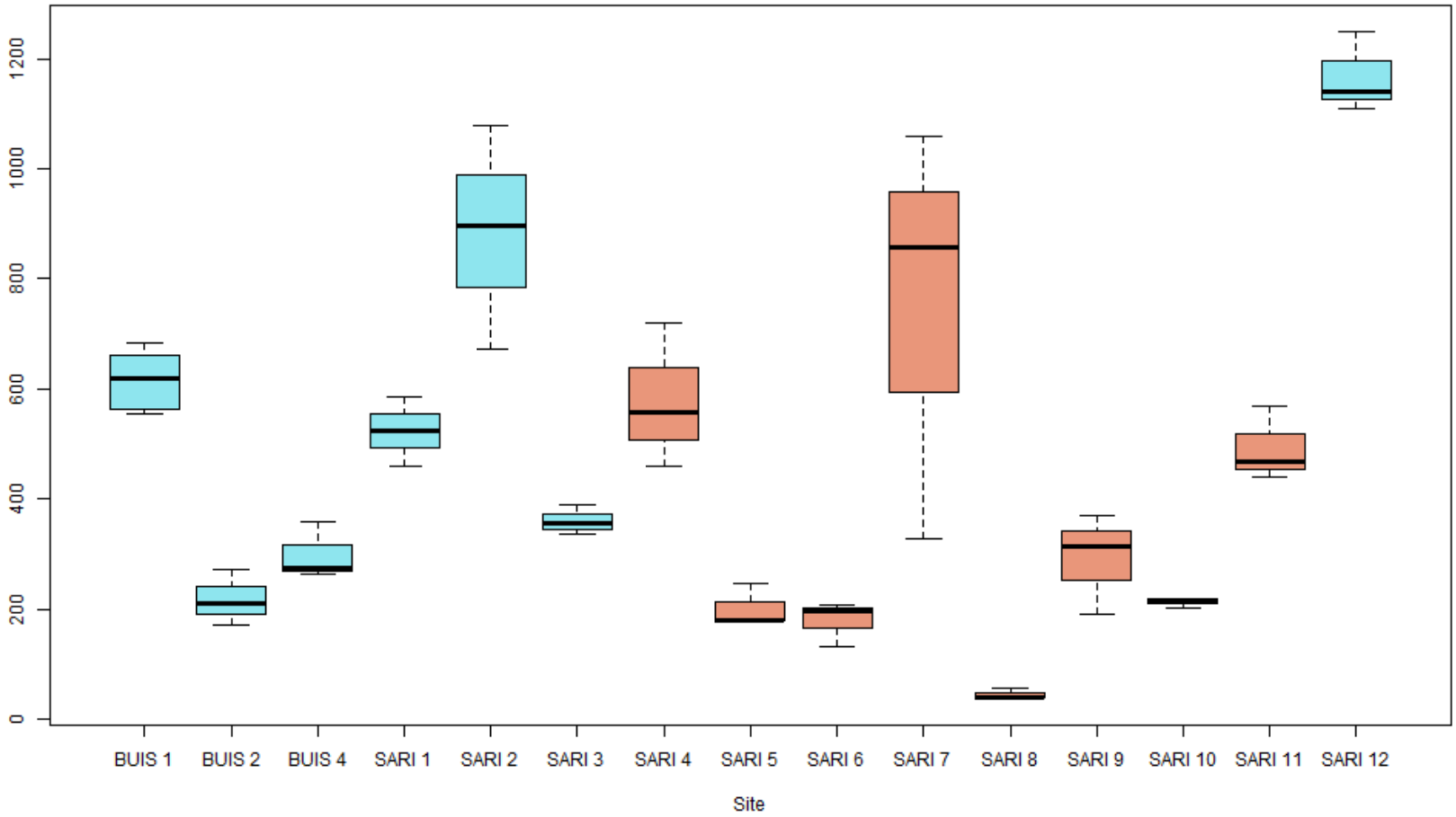

Figure 3. Boxplots of median grain size by SARI and BUIS site. The median grain size of the volume distribution was measured using a laser diffraction particle size analyzer, and the median values from three replicates at each site were used for the boxplot. Sites in blue are reef sites with *A. palmata* coral and sites in pink are estuary sites. Sites with significant differences according to Tukey's HSD do not contain any corresponding letters ($p < 0.05$).

Table 2. SARI and BUIS sediment size classifications. Sediment grain size classifications were determined from the average volume particle size distributions from three sediment replicates [± SD]. The sediment classification categories and sizes were based on USDA (1987).

Site	**% Clay** (< 0.002 mm)	**% Silt** (0.002 mm to 0.05 mm)	**% Very Fine Sand to Coarse Sand** (0.05 mm to 1.0 mm)	**% Very Coarse Sand to Gravel** (> 1 mm)
SARI 1	0.01 ± 0.02	3.13 ± 0.74	93.5 ± 1.89	3.36 ± 1.85
SARI 2	< 0.01	0.33 ± 0.43	25.8 ± 31.9	73.9 ± 32.3
SARI 3	0.08 ± 0.14	2.01 ± 0.25	89.5 ± 2.67	8.44 ± 2.52
SARI 4	0.65 ± 0.21	5.03 ± 1.22	65.7 ± 2.74	28.6 ± 3.72
SARI 5	0.91 ± 0.41	9.57 ± 3.11	75.5 ± 10.0	14.0 ± 13.3
SARI 6	0.39 ± 0.68	7.77 ± 5.65	50.8 ± 11.5	41.0 ± 6.66
SARI 7	0.07 ± 0.13	1.54 ± 2.42	49.5 ± 24.1	48.9 ± 21.9
SARI 8	2.33 ± 0.55	35.8 ± 5.25	32.7 ± 4.72	29.2 ± 6.06
SARI 9	0.61 ± 0.47	6.71 ± 3.41	50.1 ± 4.13	42.5 ± 7.90
SARI 10	0.09 ± 0.15	4.82 ± 2.14	85.1 ± 1.97	9.99 ± 2.12
SARI 11	< 0.01	1.98 ± 0.40	66.8 ± 0.81	31.2 ± 0.67
SARI 12	< 0.01	< 0.01	18.2 ± 4.18	81.8 ± 4.18
BUIS 1	< 0.01	2.35 ± 0.37	70.0 ± 0.28	27.6 ± 0.65
BUIS 2	0.11 ± 0.11	7.61 ± 1.75	89.3 ± 1.67	3.03 ± 0.36
BUIS 4	< 0.01	1.67 ± 0.37	97.1 ± 0.35	1.21 ± 0.70

3.3 Coral Skeleton Elemental Analysis

Coral skeletons were analyzed to determine uptake of bioavailable elements from the water column as an indication of exposure. The summary statistics of the 26 elements measured in the *A. palmata* coral skeletons (µg/g) were calculated from pooled data that was collected on colony samples from each site (Table 3). Trace element mass fractions and ratios to Ca (X/Ca) for each site are listed in Table S8 and Table S9. When comparing *A. palmata* by park, Zn/Ca and Pb/Ca ratios were significantly greater in SARI than BUIS coral skeletons, while B/Ca, P/Ca, Cd/Ca and Ba/Ca ratios were significantly greater in BUIS than SARI coral skeletons ($p < 0.05$). While Cu was one of the heavy metals elevated in SARI sediment, it did not appear significantly greater in SARI coral. Copper has a low bioaccumulation factor in other coral species (*H. microconos, F. speciosa, P. lobata*), and had the lowest assimilation of metals analyzed in other studies (Ali *et al.*, 2011; Mohammed and Dar, 2009; Mokhtar *et al.*, 2012). Howard and Brown (1984) suggest Cu is one of the elements discriminated against during element substitution, which they determined from its divalent ionic radius and electronegativity.

Table 3. Summary statistics for trace elements in coral skeleton. All mass fractions are in µg/g dry mass fraction, except Ca is expressed as a percentage.

	SARI					BUIS				
Element	Mean	± SE	Median	Min	Max	Mean	± SE	Median	Min	Max
Li	0.42	0.01	0.41	0.40	0.45	0.41	0.01	0.41	0.39	0.43
B	55.1	1.32	55.9	52.5	56.8	63.4	0.78	63.5	61.5	65.0
Na	3972	51.5	3941	3903	4073	4255	44.5	4258	4152	4353
Mg	1164	27.1	1170	1114	1208	1224	43.0	1237	1108	1315
Al	6.39	0.28	6.21	6.02	6.94	6.43	0.74	6.42	4.76	8.12
P	33.8	2.31	31.5	31.5	38.4	50.8	2.91	52.2	42.6	56.2
Ca %	39.2	1.59	38.8	36.7	42.1	39.0	0.80	39.0	36.9	40.9
V	0.04	< 0.01	0.04	0.04	0.04	0.04	< 0.01	0.04	0.04	0.04
Cr	0.08	0.05	0.05	0.01	0.18	0.04	0.02	0.04	0.01	0.08
Mn	0.64	0.14	0.53	0.48	0.91	0.49	0.02	0.47	0.46	0.55
Fe	6.43	2.68	3.81	3.70	11.8	4.19	0.72	4.33	2.38	5.74
Co	0.14	< 0.01	0.14	0.14	0.14	0.14	< 0.01	0.14	0.14	0.14
Ni	0.51	0.04	0.48	0.46	0.60	0.51	0.03	0.52	0.42	0.57
Cu	0.25	0.04	0.22	0.20	0.34	0.18	0.02	0.17	0.14	0.24
Zn	3.43	0.66	3.32	2.34	4.63	1.71	0.45	1.51	0.91	2.91
Rb	0.01	< 0.01	0.01	0.01	0.01	0.01	< 0.01	0.01	0.01	0.01
Sr	7727	63.3	7729	7617	7836	7838	59.1	7831	7727	7964
Mo	0.08	0.04	0.05	0.04	0.16	0.72	0.28	0.70	0.05	1.44
Ag	0.01	< 0.01	0.01	0.01	0.01	0.01	< 0.01	0.01	0.01	0.01
Cd	0.08	0.01	0.07	0.07	0.09	0.10	< 0.01	0.09	0.09	0.10
Sb	0.01	< 0.01	0.01	0.01	0.02	0.01	< 0.01	0.01	0.01	0.01
Cs	< 0.01	< 0.01	< 0.01	< 0.01	< 0.01	< 0.01	< 0.01	< 0.01	< 0.01	< 0.01
Ba	21.6	1.15	22.1	19.4	23.2	36.4	3.32	36.6	28.2	44.4
Nd	0.01	< 0.01	0.01	< 0.01	0.01	0.01	< 0.01	0.01	0.01	0.01
Pb	0.04	< 0.01	0.04	0.04	0.05	0.03	< 0.01	0.03	0.03	0.04
U	2.86	0.04	2.89	2.79	2.90	2.80	0.06	2.80	2.65	2.94

Elements analyzed in the *A. palmata* skeleton, particularly heavy metals, were low compared to other studies that measured elements in different coral species (Table 4), but these comparisons should be interpreted with caution because methodology varied between studies (Table S10). The biggest influence on results could be attributed to whether quality assurance (QA) and quality control (QC) measures were implemented in the studies. Without the specified use of internal standards, calibration curves, controls, reference materials, and procedural blanks, concentrations may be overestimated. Additional methodology differences were noted in the organic material removal and the procedure used for skeletal digestion. The initial removal of organic material (tissue and zooxanthellae) differed, which may affect the efficacy of completely removing all organic matter prior to dissolution of the skeleton. Some studies rinsed the skeleton with acid prior to digestion, which may have dissolved some of the skeleton. Furthermore, whether the skeleton and tissue were in whole pieces or ground (and the size of ground material) for each of the steps may affect whether the organic material from the skeletal matrix and any obtrusions were removed or included in the analysis. Acid strengths were greater in some of the other studies, but the steps taken prior to dissolution of the skeleton likely contributed more to concentration differences because the 2 % HNO_3 used in this study appeared to completely dissolve the skeleton and left no particulates remaining.

Despite methodology differences, inter-reef and inter-species comparisons can provide valuable insight. The mass fraction comparisons in Table 4 show two sites with varying degrees of contamination

(Guzmán and Jiménez, 1992), two sites with varying distance from riverine/terrestrial input (Bastidas and García, 1999), two sites with an *Acropora* species (Reichelt-Brushett and McOrist, 2003), and multiple coral species within the same location (Jiang *et al.*, 2020; Mokhtar *et al.*, 2012). All studies analyzed species other than *A. palmata*. The seawater-skeleton partitioning coefficients for metals have been shown to vary among species (Jiang *et al.*, 2020), which would result in the observed difference in skeletal element mass fractions among species, including those at the same site (Ali *et al.*, 2011; Esslemont, 2000; Glynn *et al.*, 1989). Esslemont (2000) also showed differences in the amount of metals partitioned in the tissue compared to the skeleton for *Goniastria aspera*, *Pocillopora damicornis*, and *Acropora formosa*. Partitioning differences among species can be attributed to varying tolerance of metals and the zooxanthellae density in the coral tissue (Esslemont, 2000). The difference in metal tolerance is likely related to the coral's ability to metabolize, efflux, or transform these elements before offloading to the skeleton or perhaps the zooxanthellae's ability to accumulate metals and their density in the tissue. Zooxanthellae accumulate trace metals at greater concentrations than the coral tissue in *A. tenuis, A. formosa, P. damicornis,* and *Porites spp* (Reichelt-Brushett and McOrist, 2003; Shah, 2008). Their density in the tissue would change the concentration that would be transferred to tissue and skeleton, particularly with exposure to increased metals or additional stressors causing zooxanthellae to be expelled. Differences in bioaccumulation also may be attributed to skeletal shape and structure. Anu *et al.* (2007) found greater metal concentrations in skeleton and tissue of ramose and branching coral. However, many of the species with greater mass fractions of metals than *A. palmata* were rounded, lobed, or boulder-like and have a distinct structure from *A. palmata* with its large branches. *Acropora palmata* has a perforate skeleton and other species, such as *Porites spp*., have imperforate skeletons, which might affect trace element transfer. Ultimately, *A. palmata* appeared to have lower concentrations of metals in the skeleton when compared to these other studies. This does not suggest *A. palmata* was exposed to lower environmental concentrations or that the exposure level was less toxic in the current study since as these studies have shown, skeletal metal concentrations can vary with many factors: species, skeletal morphology differences, variation in coral components (*e.g.* zooxanthellae density), and the presence of underlying stressors. It also is difficult to compare between studies with differing methodological techniques and without the specified use of QA/QC methods. Therefore, the best comparison, discussed below, is between *A. palmata* skeletons at SARI and BUIS to examine how metal exposure and physico-chemical water quality parameters might relate to the previously observed biological health differences between sites.

Table 4. Coral skeleton trace element analysis comparisons across studies. All reported values are dry mass fractions in µg/g ± standard deviation ([-] = not measured; ND = not detected). Mass fractions are shown as either averages or ranges.

	Location	Species	Al	Cd	Cr	Cu	Fe	Mn	Ni	Pb	V	Zn
1	Costa Rica	*Siderastrea siderea*	313 ± 35.2	7.5 ± 0.1	7.3 ± 0.7	2.0 ± 0.1	113.2 ± 17.6	7.3 ± 0.7	91.6 ± 2.9	-	44.7 ± 3.9	10.2 ± 1.3
	Panama		250.7 ± 29.1	7.6 ± 0.0	9.9 ± 1.7	3.8 ± 0.6	70.8 ± 7.3	6.9 ± 1.3	93.7 ± 3.5	-	41.8 ± 1.7	8.9 ± 0.8
2	Punta Brava, Venezuela	*Porites astreoides*	139.29 ± 203.66	-	0.797 ± 0.084	16.33 ± 1.56	62.05 ± 10.96	-	-	0.208 ± 0.059	0.315 ± 0.051	10.67 ± 0.84
	Bajo Caiman, Venezuela		13.88 ± 2.374	-	1.952 ± 0.575	12.52 ± 0.84	18.09 ± 2.34	-	-	1.037 ± 0.203	0.262 ± 0.041	9.12 ± 0.706
3	Magnetic Island, Australia	*Acropora tenuis*	-	0.001	-	0.08	16.3	0.12	0.9	0.45	-	1.15
	One Tree Island, Australia		-	<0.001	-	0.055	ND	0.015	0.45	0.01	-	0.25
4	Sabah, Malaysia	*Hydnophora microconos*	-	1.5 ± 0.05 to 2.2 ± 0.11	-	6.2 ± 0.45 to 9.2 ± 0.46	11 ± 0.65 to 64 ± 4.1	5.9 ± 0.47 to 14 ± 1.2	21 ± 0.48 to 26 ± 0.85	-	-	1.9 ± 0.27 to 5.6 ± 0.16
		Favia speciosa	-	1.4 ± 0.38 to 2.2 ± 0.09	-	6.7 ± 0.46 to 11 ± 1.2	14 ± 0.64 to 57 ± 3.5	6.0 ± 0.18 to 13 ± 1.1	18 ± 0.78 to 25 ± 0.48	-	-	1.6 ± 0.06 to 7.8 ± 0.71
		Porites lobata	-	0.74 ± 0.21 to 2.0 ± 0.14	-	6.2 ± 0.47 to 7.7 ± 1.3	13 ± 1.7 to 62 ± 6.8	4.4 ± 0.45 to 12 ± 0.87	16 ± 0.48 to 25 ± 1.3	-	-	2.5 ± 0.36 to 5.8 ± 0.36
5	Weizhou Island, China	*Favia palauensis*	-	0.16	0.98	3.74	-	-	-	1.52	-	27.7
		Porites lutea	-	0.09	0.72	2.70	-	-	-	1.58	-	19.2
		Pavona decussata	-	0.15	0.54	2.52	-	-	-	2.51	-	17.6
6	SARI, St. Croix, USVI	*Acropora palmata*	6.02 ± 2.22 to 6.94 ± 1.55	0.07 ± 0.03 to 0.09 ± 0.06	0.01 ± 0.02 to 0.18 ± 0.51	0.20 ± 0.10 to 0.34 ± 0.41	3.70 ± 2.25 to 11.8 ± 20.0	0.48 ± 0.10 to 0.91 ± 1.26	0.46 ± 0.05 to 0.60 ± 0.41	0.04 ± 0.00 to 0.05 ± 0.01	0.04 ± 0.00 to 0.04 ± 0.01	2.34 ± 0.95 to 4.63 ± 1.93
	BUIS, St. Croix, USVI		4.76 ± 2.41 to 8.12 ± 2.27	0.09 ± 0.03 to 0.10 ± 0.04	0.01 ± 0.01 to 0.08 ± 0.12	0.14 ± 0.03 to 0.24 ± 0.22	2.38 ± 1.08 to 5.74 ± 4.72	0.46 ± 0.13 to 0.55 ± 0.13	0.42 ± 0.03 to 0.57 ± 0.24	0.03 ± 0.01 to 0.04 ± 0.02	0.04 ± 0.00 to 0.04 ± 0.01	0.91 ± 0.62 to 2.91 ± 2.29

Sources: [1]Guzman and Jimenez, 1992; [2]Bastidas and Garcia, 1999; [3]Reichelt-Brushett and McOrist, 2003; [4]Mokhtar *et al.*, 2012; [5]Jiang *et al.*, 2020; [6]Current Study

3.3.1 Elements Greater in SARI A. palmata Skeleton (Zn, Pb)

Acropora palmata coral skeletons in SARI contained significantly greater Zn and Pb when compared to BUIS. Zinc has exhibited the greatest bioaccumulation factor when compared to Mn, Ni, Fe, Cd, and Cu in *Hydnophora microconos*, *Favia speciosa*, and *Porites lobata* (Mokhtar *et al.*, 2012). Zinc is essential for coral growth and calcification (Ferrier-Pagès *et al.*, 2005; Houlbrèque *et al.*, 2012), but has been shown to decrease coral fertilization rates at seawater concentrations 10 µg/L Zn ($ZnSO_4$) or greater (Reichelt-Brushett and Harrison, 2005). Lead, which is not a micronutrient for coral, can also decrease fertilization rates at elevated concentrations in seawater (1352 µg/L to 2400 µg/L Pb) as $Pb(NO_3)_2$ (Reichelt-Brushett and Harrison, 2005), though these concentrations are greater than what has been measured in sewage polluted coastal water (150 ng/kg total Pb) (Patterson *et al.*, 1976). Zinc and Pb are typically the most concentrated metals found in urban stormwater runoff (Davis *et al.*, 2001). They are commonly derived from residential areas since they are used in siding material for buildings (Davis *et al.*, 2001). Zinc is also used in tire production and becomes a byproduct of tire-wear (Councell *et al.*, 2004). Since Zn and Pb were greater in coral at SARI than BUIS, the coral in the SARI watershed are likely being exposed to a greater anthropogenic influence, particularly commercial and residential development and stormwater.

3.3.2 Elements Greater in BUIS A. palmata Skeleton (B, P, Cd, Ba)

Acropora palmata skeletons in BUIS exhibited significantly greater B, P, Cd, and Ba when compared to SARI. Boron, a proxy for pH or calcification chemistry, is incorporated into coral aragonite by borate $B(OH)_4^-$ substitution with carbonate CO_3^{2-} (Fowell *et al.*, 2018). The speciation of $B(OH)_4^-$ versus boric acid is pH driven, so B mass fractions in the coral skeleton typically reflect pH differences in the water column (Klochko *et al.*, 2006). However, understanding the actual pH trends requires measurement of boron isotope ratios and, even then, interpretation can be very complex due to the changes in pH occurring in the calcifying fluid (DeCarlo *et al.*, 2018; Fowell *et al.*, 2018). Yet, the greater B signature at BUIS than SARI, indicating a greater pH at BUIS, mirrors historical differences in pH measurements at these parks. SARI has been listed as impaired for low pH measurements (< 6.7 pH), while BUIS has not exhibited any pH impairments (7.0 – 8.3 pH) (DPNR, 2018). Low pH can be derived from freshwater inputs, which often have a lower pH than seawater, or from higher biological respiration rates combined with the lower mixing rates (Feely *et al.*, 2010).

Phosphorus (P) is a nutrient and the concentration in coral skeleton can be used to assess nutrient levels in the surrounding seawater. Sediment porewater from SARI and BUIS analyzed by May and Woodley (2016) also contained greater concentrations of inorganic P at BUIS (up to 367.0 µg/L) compared to SARI (up to 121.0 µg/L). However, sediment composition at SARI and BUIS do not reflect the availability of P. The sediment at BUIS consisted of greater $CaCO_3$, which readily binds inorganic P, rendering it less bioavailable to organisms (Jensen *et al.*, 1998). Sediment in SARI, much lower in $CaCO_3$, has more available P due to greater P dissolution. The SARI watershed is also more likely to experience increased P from nutrient runoff, so the source at BUIS causing greater mass fractions of P in the coral skeletons is difficult to identify. Phosphorus can be derived from upwelling. LaVigne *et al.* (2008) observed that greater P/Ca was associated with seasonal upwelling in the Gulf of Panamá when tracking the mass fractions in *Pavona gigantea* coral skeleton. Chérubin and Garavelli (2016) describe a potential small source of upwelling near the shore of St. Croix. Another explanation for greater P in *A. palmata* skeletons at BUIS is that seabird populations excrete waste enriched in P, which reaches the reefs; however, the $\delta^{15}N$ signature does not align with this theory. Lorrain *et al.* (2017) saw a much greater $\delta^{15}N$ signature when seabirds were present, even with distance from shore, due to N supply from seabird waste. The $\delta^{15}N$ at BUIS is too low to indicate a nutrient contribution from bird waste. Thus,

sources of P at BUIS may be derived from another nearby watershed, nutrients transported via the Amazon freshwater plume, which is discussed below with Ba, or from upwelling.

Cadmium (Cd), a known potentially toxic heavy metal, has the greatest mass fractions (97 ng/g ± 14 ng/g (SE)) observed in the coral skeleton at BUIS 2. Greater mass fractions of Cd can be derived from natural or anthropogenic sources. Coral skeleton Cd/Ca is a proxy for upwelling since Cd is more abundant in cold, deep, nutrient-rich water and can quickly be depleted at the surface from biological activity (Shen *et al.,* 1987). Alternatively, skeletal Cd/Ca mass fractions increase from urban and industrial input. However, the lack of urban and industrial input at BUIS and the greater coral skeleton mass fraction of P/Ca and Ba/Ca at BUIS points to upwelling as an influence on the elevated trace elements found in the coral skeletons at BUIS.

Barium often indicates freshwater exposure in $CaCO_3$ structures (Elsdon and Gillanders, 2006; Macdonald and Crook, 2010; Moyer *et al.,* 2012). At low salinities (0 mg/g to 5 mg/g), Ba is desorbed from clay making it naturally more abundant in freshwater (Li and Chan, 1979), but there is no natural source of freshwater on Buck Island. However, studies mention that Orinoco and Amazon River freshwater has a seasonal influence on the Caribbean (Chérubin and Garavelli, 2016; Johns *et al.,* 2014). Climatology maps show the decrease in salinity (approximately 0.4 ppt) that occurs in St. Croix after the flood season and show a specific island mass effect that occurs when the current reaches St. Croix and flows around both the north and south side of the island (Chérubin and Garavelli, 2016). The Orinoco and Amazon River are responsible for about 20 % of the world's riverine input, so these freshwater plumes have an impact on the Caribbean's salinity, temperature, chlorophyll, and dissolved oxygen levels (Johns *et al.,* 2014), which suggests they may impact nutrient input as well. Greater Ba signatures can also reflect a natural source of upwelling since Ba is more abundant in cold, deep water versus warm, surface water (Lea *et al.,* 1989). Chérubin and Garavelli (2016) described a type of potential upwelling in St. Croix caused by north coast trade winds. Salinity trends reflected isopycnals near the coast that would be upwelled and transported offshore delivering colder and deeper water to the north of St. Croix where Buck Island lies (Chérubin and Garavelli, 2016), but this source of upwelling would be relatively small. The greater mass fraction of both P and Ba at BUIS supports the idea that either upwelling or an external eutrophic freshwater source is reaching BUIS.

3.4 Stable Isotope Analysis

Stable isotopes were analyzed in the coral tissue to help interpret the sources (*e.g.* anthropogenic, terrestrial, oceanic) of trace elements measured in sediment and coral, and to validate findings. Coral $\delta^{13}C$ and $\delta^{15}N$ ranged from -17.14 ‰ to -11.32 ‰ and 0.13 ‰ to 2.61 ‰, respectively. The statistical analysis of the stable isotopes across all sites revealed that $\delta^{13}C$ was significantly lower at SARI 1 when compared to SARI 2 and SARI 3 ($p < 0.05$) (Figure 4). The $\delta^{15}N$ displayed no significant differences by site within SARI, and there were no differences in $\delta^{13}C$ or $\delta^{15}N$ among sites within BUIS. When comparing *A. palmata* between parks, $\delta^{13}C$ and $\delta^{15}N$ were both lower at SARI than at BUIS ($p < 0.001$) (Figure 4).

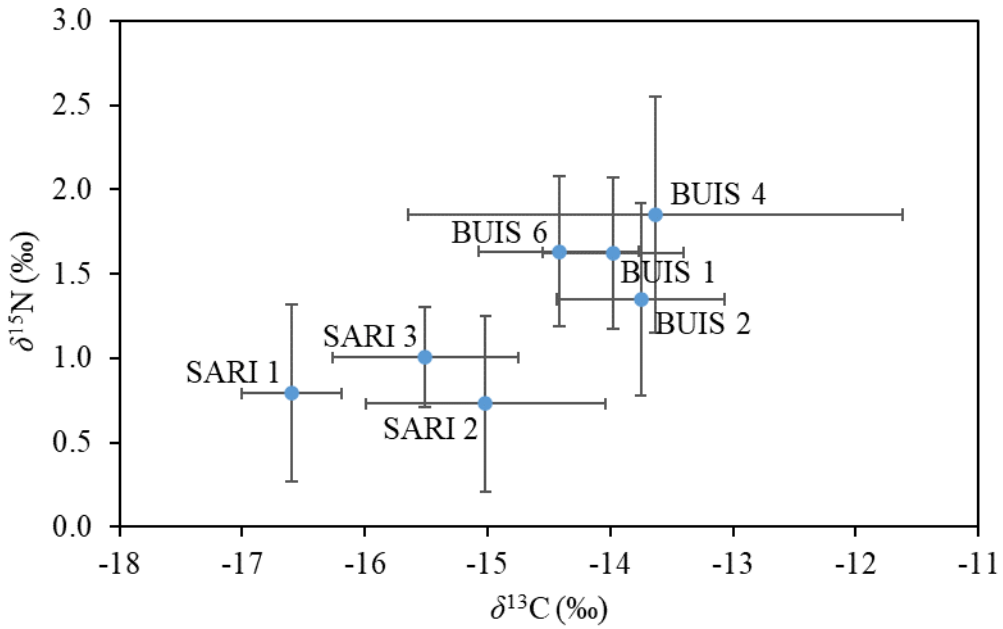

Figure 4. δ^{15}N and δ^{13}C isotope signatures by SARI and BUIS site. δ^{15}N and δ^{13}C (mean ± standard deviation) were measured in the tissue from *A. palmata* biopsies. Ten tissue samples were analyzed from each site, except BUIS 4 (n = 3).

The δ^{13}C in the coral tissue displayed ranges comparable to other studies, but the δ^{15}N was low compared to other studies throughout the Caribbean and in other regions of the world (Heikoop *et al.*, 2000; Hoegh-Guldberg *et al.*, 2004; Muscatine *et al.*, 2005; Sammarco *et al.*, 1999; Wang *et al.*, 2015; Yamamuro *et al.*, 1995). A study in Jamaica analyzed δ^{15}N in *Montastraea annularis, Porites astreoides, and Agaricia agaricites* tissue, and *A. palmata* tissue from BUIS contained similar δ^{15}N values to those analyzed at 10 m depth, but δ^{15}N in SARI coral tissue was still lower (below 1.5 ‰ δ^{15}N) (Heikoop *et al.*, 1998). Interspecies δ^{15}N variation has been shown within the same site, but inter-reef δ^{15}N variability appears greater (Heikoop *et al.*, 2000, 1998). Sampling and processing methodology may also contribute to δ^{15}N differences between studies. Some studies did not specify sampling location on the coral colony. The base of the coral has lower photosynthetically active radiation (PAR) than the top of the coral, and PAR is correlated to the coral's δ^{15}N (Heikoop *et al.*, 1998). Additionally, PAR is seasonal, and all studies did not collect samples at the same time of year. Sample cleaning techniques, the decalcification process, and whether coral skeleton was ground or whole prior to the decalcification process may also influence the tissue and zooxanthellae nitrogen recovery.

The lower δ^{13}C found in coral tissue at SARI when compared to BUIS indicates SARI coral are exposed to a greater amount of carbon derived from terrestrial sources. The coral measured at BUIS is also further from shore than the SARI coral. Sammarco *et al.* (1999) showed that δ^{13}C in tissue increased with distance from shore in *Porites lobata*. The distance from shore may simply coincide with a lower influence of terrestrial carbon sources, which have lower δ^{13}C. The greater δ^{13}C at BUIS also could a indicate that the coral at BUIS have higher primary productivity compared to SARI. The organic carbon consumed during heterotrophic feeding has a lower δ^{13}C signature than the inorganic carbon that is assimilated during autotrophic feeding (δ^{13}C -14 to -10‰) (as summarized by Heikoop *et al.*, 2000). Lower primary productivity in SARI coral and a greater terrestrial input in the SARI watershed coincides with the results found for δ^{15}N.

Acropora palmata tissue from SARI also displayed a significantly lower δ^{15}N than the coral tissue at BUIS and in St. Croix overall compared to other studies. Since terrestrial nitrogen is more depleted in ^{15}N than marine nitrogen, lower δ^{15}N could be the result of a greater natural terrestrial influence at SARI (Owens and Law, 1989). Adding inorganic nutrients (ammonium and phosphate) can lower δ^{15}N from 3-4 ‰ to 1 ‰ (Hoegh-Guldberg *et al.,* 2004). Nutrient availability may be greater at SARI resulting in a low δ^{15}N when compared to BUIS. Along with natural terrestrial sources, terrestrial runoff may also include synthetic fertilizer (-4 ‰ to + 4 ‰ δ^{15}N) comprised of atmospheric nitrogen, which is deplete of ^{15}N (Hoefs, 2015).

Other terrestrial sources contributing to the lower δ^{15}N values could include a variety of nitrogen inputs and nitrogen cycle processes. Lower δ^{15}N may result from an increase in heterotrophic feeding (Brenner *et al.,* 1999) and a decrease in symbiont photosynthesis (autotrophic feeding) in coral, which can be influenced by depth and light attenuation. Heikoop *et al.* (1998) showed that as depth increased, δ^{15}N ‰ decreased in coral tissue of multiple species. The δ^{15}N decrease was also significantly correlated with an increase in attenuated light. In summary, many sources may contribute to the lower δ^{15}N at SARI, but the main influences can be summarized as terrestrial sources, nitrogen fixation, and a difference in food source and availability. Coral also have a complex internal nitrogen cycle within the holobiont that is not completely understood and could be contributing to some of the minor isotopic differences between sites (Rädecker *et al.,* 2015).

The low δ^{15}N signature in the tissue indicates *A. palmata* was not exposed to a substantial amount of treated wastewater. In a study by Risk *et al.* (2009) coral tissue that has been exposed to wastewater displayed δ^{15}N up to 7.3 ‰, whereas the greatest δ^{15}N in tissue from St. Croix was 1.85 ‰ (BUIS 4). However, raw sewage can have a low δ^{15}N in contrast to treated wastewater (Rogers, 2003). Raw sewage is more elevated in ammonia while treated wastewater contains mostly nitrate and nitrite. More evidence is available to support raw sewage as the source of low δ^{15}N; the Waste Management Authority pump station in Christiansted (Figure 1), upstream of the SARI reef sites, has been known to overflow during heavy rain events and cause spikes in fecal associated bacteria (up to 78,000 total coliforms MPN/100 mL; MPN = most probable number) in the surface water near Christiansted Harbor (National Water Quality Monitoring Council, 2019). Fecal associated bacteria also have been out of compliance with water quality criteria at sites outside of the Christiansted Harbor and in SARI from 2010 to 2018 (DPNR, 2018). Bacteria is likely transported from Christiansted to SARI by the longshore current (Figure 1), which flows east to west and is pushed by the easterly trade winds (Kendall *et al.*, 2005).

4. Conclusions

This study provides a critical framework for examining the causative agents that may be impacting environmental health at SARI and BUIS, as well as likely sources impairing biological processes in coral at these sites. Sediment Cu was elevated at four sites in SARI with values above the ERL (Long *et al.,* 1995), so this heavy metal should be monitored and further explored for direct biological impact. Major sources are likely boat building and marina activities including those associated with the Christiansted Harbor, upstream of SARI. *Acropora palmata* in SARI also demonstrated greater exposure to terrestrial sources, such as inorganic nutrients and/or raw sewage, interpreted from the low δ^{15}N. One known source of sewage is the Christiansted Harbor pump station, which is possibly contributing to the low δ^{15}N signature in SARI. In addition to fecal associated bacteria, wastewater can introduce nutrients, surfactants, metals and other harmful chemicals. Thus, the wastewater overflow may be a source of metals and other observed water quality changes. The greater mass fractions of Zn and Pb in SARI coral skeletons compared to BUIS provides additional evidence that this overflow is reaching the SARI reef sites because the pump station is a combined stormwater and sewage system, and Zn and Pb

are typically the most abundant metals in stormwater (Davis *et al.,* 2001). Furthermore, SARI 1 corals were exposed to the greatest amount of carbon derived from terrestrial/anthropogenic sources. SARI 1 is the site in closest proximity to Christiansted and the Judith's Fancy housing development. This suggests that a greater terrestrial input is reaching the SARI coral from these sources than from the Salt River Bay. The trace element analyses in the skeleton indicated that elements available to BUIS coral (P, Cd, and Ba) may be derived from an upwelling or freshwater source; however, nutrients and metals, like P and Cd, can be transported in wastewater and should not be eliminated as a potential input to the BUIS reefs.

This investigation will be valuable to the National Park Service and to the Department of Planning and National Resources because it identifies potential threats to the health of the parks and to coral recovery. These threats should be further analyzed to identify direct impacts on local species in order to successfully implement management strategies that would preserve *A. palmata* and assist with recovery from its threatened status. Additional analyses might include seawater sampling to determine the bioavailable concentrations of metals. Sediment samples could also be collected via sediment traps during the wet season to determine the level of sedimentation as well as the concentrations of heavy metals in re-suspended sediment, which acts as a source of exposure to coral. Sequential leaching methods could be applied to the sediment, which isolates the different phases of metals and reveals which metals were introduced to the environment via pollution (Hou *et al.,* 2013; Tessier *et al.,* 1979). Samples should be taken during the wet season, particularly in coral tissue, to look at real-time uptake of heavy metals and sewage signatures. Biotracers could also be used in sewage to track the sewage and stormwater overflow to see how quickly it reaches the coral and how much is transferred. The findings in the current study will also be used to examine the correlation of the water quality data with *A. palmata* reproductive pathologies, which are currently being analyzed, to see if heavy metals or other trace element proxies are correlated with reproductive failure at SARI and BUIS.

Funding

This work was supported by the NOAA Coral Reef Conservation Program [Project # 31144].

Acknowledgments

We thank the National Park Service in St. Croix for providing SCUBA diving support during sampling. We also thank Jay Brandes at the Skidaway Institute Scientific Stable Isotope Laboratory (Savannah, GA) for analyzing stable isotopes in the coral samples.

Conflicts of Interest

None

NIST Disclaimer

Any mention of commercial products is to specify adequately the analytical procedures used. It does not imply recommendation or endorsement by NIST, or that the products mentioned are necessarily the best available for the intended purpose. Employment of the sample digestion procedures outlined would expose analysts to hydrofluoric, hydrochloric and nitric acids; appropriate personal protective equipment should be used if these methods are adopted for sample preparation.

References

Acevedo-Figueroa, D., Jiménez, B.D., Rodríguez-Sierra, C.J., 2006. Trace metals in sediments of two estuarine lagoons from Puerto Rico. Environ. Pollut. 141, 336–342. https://doi.org/10.1016/j.envpol.2005.08.037

Al-Rousan, S., Al-Shloul, R., Al-Horani, F., Abu-Hilal, A., 2012. Heavy metals signature of human activities recorded in coral skeletons along the Jordanian coast of the Gulf of Aqaba, Red Sea. Environ. Earth Sci. 67, 2003–2013. https://doi.org/10.1007/s12665-012-1640-0

Al-Rousan, S.A., Al-Shloul, R.N., Al-Horani, F.A., Abu-Hilal, A.H., 2007. Heavy metal contents in growth bands of Porites corals: Record of anthropogenic and human developments from the Jordanian Gulf of Aqaba. Mar. Pollut. Bull. 54, 1912–1922. https://doi.org/10.1016/j.marpolbul.2007.08.014

Ali, A.A.M., Hamed, M.A., El-Azim, H.A., 2011. Heavy metals distribution in the coral reef ecosystems of the Northern Red Sea. Helgol. Mar. Res. 65, 67–80. https://doi.org/10.1007/s10152-010-0202-7

Alminas, H. V, Foord, E.E., Tucker, R.E., 1994. Geochemistry, Mineralogy, and Geochronology of the U.S. Virgin Islands. U.S. Government Printing Office, Washington.

Anu, G., Kumar, N.C., Jayalakshmi, K.J., Nair, S.M., 2007. Monitoring of heavy metal partitioning in reef corals of Lakshadweep Archipelago, Indian Ocean. Environ. Monit. Assess. 128, 195–208. https://doi.org/10.1007/s10661-006-9305-7

ASTM, 2006. Standard Guide for Conducting Static Acute Toxicity Tests with Echinoid Embryos. West Conshohocken, PA.

Bastidas, C., García, E., 1999. Metal content on the reef coral Porites astreoides: An evaluation of river Influence and 35 years of chronology. Mar. Pollut. Bull. 38, 899–907. https://doi.org/10.1016/S0025-326X(99)00089-2

Belzile, N., Chen, Y.W., Gunn, J.M., Dixit, S.S., 2004. Sediment trace metal profiles in lakes of Killarney Park, Canada: From regional to continental influence. Environ. Pollut. 130, 239–248. https://doi.org/10.1016/j.envpol.2003.12.003

Berey, R.W., 2012. "Quick Look" Report Results from the Seawater Intake Study for the Salt River Marine Research and Educational Center.

Bernard, D., 1995. Metals in sediments from two lagoons off Guadeloupe, West Indies. Mar. Pollut. Bull. 30, 619–621. https://doi.org/10.1016/0025-326X(95)00085-2

Brenner, M., Whitmore, T.J., Curtis, J.H., Hodell, D.A., Schelske, C.L., 1999. Stable isotope (δ^{13}C and δ^{15}N) signatures of sedimented organic matter as indicators of historic lake trophic state. J. Paleolimnol. 22, 205–221. https://doi.org/10.1023/A:1008078222806

Brown, B.E., Tudhope, A.W., Le Tissier, M.D.A., Scoffin, T.P., 1991. A novel mechanism for iron incorporation into coral skeletons. Coral Reefs 10, 211–215.

Calmano, W., Hong, J., Forstner, U., 1993. Binding and mobilization of heavy metals in contaminated sediments affected by pH and redox potential. Water Sci. Technol. 28, 223–235.

Chérubin, L.M., Garavelli, L., 2016. Eastern caribbean circulation and island mass effect on St. Croix, US Virgin Islands: A mechanism for relatively consistent recruitment patterns. PLoS One 11, 1–28. https://doi.org/10.1371/journal.pone.0150409

Chiappetta, J.M.M., Machado, W., Santos, J.M., Lessa, J.A., 2016. Trace metal bioavailability in

sediments from a reference site, Ribeira Bay, Brazil. Mar. Pollut. Bull. 106, 395–399. https://doi.org/10.1016/j.marpolbul.2015.12.037

Councell, T.B., Duckenfield, K.U., Landa, E.R., Callender, E., 2004. Tire-wear particles as a source of zinc to the environment. Environ. Sci. Technol. 38, 4206–4214. https://doi.org/10.1021/es034631f

Davis, A.P., Shokouhian, M., Ni, S., 2001. Loading estimates of lead, copper, cadmium, and zinc in urban runoff from specific sources. Chemosphere 44, 997–1009.

DeCarlo, T.M., Holcomb, M., McCulloch, M.T., 2018. Reviews and syntheses: Revisiting the boron systematics of aragonite and their application to coral calcification. Biogeosciences 15, 2819–2834. https://doi.org/10.5194/bg-15-2819-2018

DPNR, 2018. USVI Integrated Water Quality Monitoring and Assessment Report. Division of Environmental Protection. Water Quality Management and Planning Program. 319 pp.

Druffel, E.R.M., 1997. Geochemistry of corals: Proxies of past ocean chemistry, ocean circulation, and climate. Proc. Natl. Acad. Sci. 94, 8354–8361. https://doi.org/10.1073/pnas.94.16.8354

Durand, A., Chase, Z., Townsend, A.T., Noble, T., Panietz, E., Goemann, K., 2016. Improved methodology for the microwave digestion of carbonate-rich environmental samples. Int. J. Environ. Anal. Chem. 96, 119–136. https://doi.org/10.1080/03067319.2015.1137904

Eakin, C.M., Morgan, J.A., Heron, S.F., Smith, T.B., Liu, G., Alvarez-Filip, L., Baca, B., Bartels, E., Bastidas, C., Bouchon, C., Brandt, M., Bruckner, A.W., Bunkley-Williams, L., Cameron, A., Causey, B.D., Chiappone, M., Christensen, T.R.L., Crabbe, M.J.C., Day, O., de la Guardia, E., Díaz-Pulido, G., DiResta, D., Gil-Agudelo, D.L., Gilliam, D.S., Ginsburg, R.N., Gore, S., Guzmán, H.M., Hendee, J.C., Hernández-Delgado, E.A., Husain, E., Jeffrey, C.F.G., Jones, R.J., Jordán-Dahlgren, E., Kaufman, L.S., Kline, D.I., Kramer, P.A., Lang, J.C., Lirman, D., Mallela, J., Manfrino, C., Maréchal, J.P., Marks, K., Mihaly, J., Miller, W.J., Mueller, E.M., Muller, E.M., Toro, C.A.O., Oxenford, H.A., Ponce-Taylor, D., Quinn, N., Ritchie, K.B., Rodríguez, S., Ramírez, A.R., Romano, S., Samhouri, J.F., Sánchez, J.A., Schmahl, G.P., Shank, B. V., Skirving, W.J., Steiner, S.C.C., Villamizar, E., Walsh, S.M., Walter, C., Weil, E., Williams, E.H., Roberson, K.W., Yusuf, Y., 2010. Caribbean corals in crisis: Record thermal stress, bleaching, and mortality in 2005. PLoS One 5, 1–9. https://doi.org/10.1371/journal.pone.0013969

Eklund, B., Eklund, D., 2014. Pleasure boatyard soils are often highly contaminated. Environ. Manage. 53, 930–946. https://doi.org/10.1007/s00267-014-0249-3

El-Sorogy, A.S., Nour, H., Essa, E., Tawfik, M., 2013. Quaternary coral reefs of the Red Sea coast, Egypt: Diagenetic sequence, isotopes and trace metals contamination. Arab. J. Geosci. 6, 4981–4991. https://doi.org/10.1007/s12517-012-0806-0

Elsdon, T.S., Gillanders, B.M., 2006. Temporal variability in strontium, calcium, barium, and manganese in estuaries: Implications for reconstructing environmental histories of fish from chemicals in calcified structures. Estuar. Coast. Shelf Sci. 66, 147–156. https://doi.org/10.1016/j.ecss.2005.08.004

Esslemont, G., 2000. Heavy metals in seawater, marine sediments and corals from the Townsville section, Great Barrier Reef Marine Park, Queensland. Mar. Chem. 71, 215–231. https://doi.org/10.1016/S0304-4203(00)00050-5

Federal Register, 2006. Endangered and Threatened Species: Final Listing Determinations for Elkhorn Coral and Staghorn Coral, 71(89), 26852-26861 (to be codified at 50 C.F.R. pt 223). https://www.federalregister.gov/documents/2006/05/09/06-4321/endangered-and-threatened-

species-final-listing-determinations-for-elkhorn-coral-and-staghorn-coral (accessed 7-7-2020)

Feely, R.A., Alin, S.R., Newton, J., Sabine, C.L., Warner, M., Devol, A., Krembs, C., Maloy, C., 2010. The combined effects of ocean acidification, mixing, and respiration on pH and carbonate saturation in an urbanized estuary. Estuar. Coast. Shelf Sci. 88, 442–449. https://doi.org/10.1016/j.ecss.2010.05.004

Ferrier-Pagès, C., Houlbrèque, F., Wyse, E., Richard, C., Allemand, D., Boisson, F., 2005. Bioaccumulation of zinc in the scleractinian coral Stylophora pistillata. Coral Reefs 24, 636–645. https://doi.org/10.1007/s00338-005-0045-x

Fisher, P., Aumann, C., Chia, K., O'Halloran, N., Chandra, S., 2017. Adequacy of laser diffraction for soil particle size analysis. PLoS One 12. https://doi.org/10.1371/journal.pone.0176510

Fowell, S.E., Foster, G.L., Ries, J.B., Castillo, K.D., de la Vega, E., Tyrrell, T., Donald, H.K., Chalk, T.B., 2018. Historical Trends in pH and Carbonate Biogeochemistry on the Belize Mesoamerican Barrier Reef System. Geophys. Res. Lett. 45, 3228–3237. https://doi.org/10.1002/2017GL076496

Fowell, S.E., Sandford, K., Stewart, J.A., Castillo, K.D., Ries, J.B., Foster, G.L., 2016. Intrareef variations in Li/Mg and Sr/Ca sea surface temperature proxies in the Caribbean reef-building coral Siderastrea siderea. Paleoceanography 31, 1315–1329. https://doi.org/10.1002/2016PA002968

Fry, B., Brand, W., Mersch, F.J., Tholke, K., Garritt, R., 1992. Automated analysis system for coupled δ^{13}C and δ^{15}N measurements. Anal. Chem. 64, 288–291. https://doi.org/10.1021/ac00027a009

Fujita, M., Ide, Y., Sato, D., Kench, P.S., Kuwahara, Y., Yokoki, H., Kayanne, H., 2013. Heavy metal contamination of coastal lagoon sediments: Fongafale Islet, Funafuti Atoll, Tuvalu. Chemosphere 95, 628–634. https://doi.org/10.1016/j.chemosphere.2013.10.023

Gardner, T.A., Coté, I.M., Gill, J.A., Grant, A., Watkinson, A.R., 2005. Hurricanes and Caribbean coral reefs: Impacts, recovery patterns, and role in long-term decline. Ecology 86, 174–184.

Gill, I.P., Hubbard, D.K., McLaughlin, P.P., Moore, C.H.J., 2004. Geology and Hydrogeology of St. Croix, Virgin Islands, in: Vacher, L.H.L., Quinn, T.M. (Eds.), Geology and Hydrogeology of Carbonate Islands. Elsevier, pp. 359–380.

Gissi, F., Stauber, J., Reichelt-Brushett, A., Harrison, P.L., Jolley, D.F., 2017. Inhibition in fertilisation of coral gametes following exposure to nickel and copper. Ecotoxicol. Environ. Saf. 145, 32–41. https://doi.org/10.1016/j.ecoenv.2017.07.009

Glynn, P.W., Szmant, A.M., Corcoran, E.E., Cofer-Shabica, S. V, 1989. Condition of Coral Reef Cnidarians from the Northern Florida Reef Tract: Pesticides, Heavy Metals, and Histopathological Examination. Mar. Pollut. Bull. 20, 568–576.

Gonzalez, H., Pomares, M., Ramirez, M., Torres, I., 1999. Heavy metals in organisms and sediments from the discharge zone of the submarine sewage outfall of Havana City, Cuba. Mar. Pollut. Bull. 38, 1048–1051. https://doi.org/10.1016/S0025-326X(99)00182-4

Guzmán, H.M., Jiménez, C.E., 1992. Contamination of coral reefs by heavy metals along the Caribbean coast of Central America (Costa Rica and Panama). Mar. Pollut. Bull. 24, 554–561. https://doi.org/10.1016/0025-326X(92)90708-E

Harris, D., Horwath, W.R., Kessel, C. van, 2001. Acid fumigation of soils to remove carbonates prior to total organic carbon or carbon-13 isotopic analysis. Soil Sci. Soc. Am. J. 65, 1853–1856.

Hedges, J.I., Stern, J.H., 1984. Carbon and nitrogen determinations of carbonate-containing solids.

Limnol. Oceanogr. 29, 657–663.

Heikoop, J.M., Dunn, J.J., Risk, M.J., Sandeman, I.M., Schwarcz, H.P., Waltho, N., 1998. Relationship between light and the δ^{15}N of coral tissue: Examples from Jamaica and Zanzibar. Limnol. Oceanogr. 43, 909–920. https://doi.org/10.4319/lo.1998.43.5.0909

Heikoop, J.M., Dunn, J.J., Risk, M.J., Tomascik, T., Schwarcz, H.P., Sandeman, I.M., Sammarco, P.W., 2000. δ^{15}N and δ^{13}C of coral tissue show significant inter-reef variation. Coral Reefs 19, 189–193. https://doi.org/10.1007/s003380000092

Hoefs, J., 2015. Stable Isotope Geochemistry, Seventh. ed. Springer International Publishing, Switzerland. https://doi.org/10.1007/978-3-319-19716-6

Hoegh-Guldberg, O., Muscatine, L., Goiran, C., Siggaard, D., Marion, G., 2004. Nutrient-induced perturbations to δ^{13}C and δ^{15}N in symbiotic dinoflagellates and their coral hosts. Mar. Ecol. Prog. Ser. 280, 105–114. https://doi.org/10.3354/meps280105

Horowitz, A.J., Elrick, K.A., 1987. The relation of stream sediment surface area, grain size and composition to trace element chemistry. Appl. Geochemistry 2, 437–451.

Hou, D., He, J., Lü, C., Ren, L., Fan, Q., Wang, J., Xie, Z., 2013. Distribution characteristics and potential ecological risk assessment of heavy metals (Cu, Pb, Zn, Cd) in water and sediments from Lake Dalinouer, China. Ecotoxicol. Environ. Saf. 93, 135–144. https://doi.org/10.1016/j.ecoenv.2013.03.012

Houlbrèque, F., Rodolfo-Metalpa, R., Jeffree, R., Oberhänsli, F., Teyssié, J.L., Boisson, F., Al-Trabeen, K., Ferrier-Pagès, C., 2012. Effects of increased pCO 2 on zinc uptake and calcification in the tropical coral Stylophora pistillata. Coral Reefs 31, 101–109. https://doi.org/10.1007/s00338-011-0819-2

Howard, L.S., Brown, B.E., 1984. Heavy Metals and Reef Corals, in: Barnes, H., Barnes, M. (Eds.), Oceanography and Marine Biology, An Annual Review, Volume 22. Aberdeen University Press, Aberdeen, UK, pp. 192–208.

Hubbard, D.K., 1992. Hurricane induced sediment transport in open-shelf tropical systems -- An example from St. Croix, U.S. Virgin Islands. J. Sediment. Petrol. 62, 946–960.

Jaffé, R., Gardinali, P.R., Cai, Y., Sudburry, A., Fernandez, A., Hay, B.J., 2003. Organic compounds and trace metals of anthropogenic origin in sediments from Montego Bay, Jamaica: Assessment of sources and distribution pathways. Environ. Pollut. 123, 291–299. https://doi.org/10.1016/S0269-7491(02)00368-8

Jensen, H.S., McGlathery, K.J., Marino, R., Howarth, R.W., 1998. Forms and availability of sediment phosphorus in carbonate sand of Bermuda seagrass beds. Limnol. Oceanogr. 43, 799–810. https://doi.org/10.4319/lo.1998.43.5.0799

Jiang, W., Yu, K., Wang, N., Yang, Hua, Yang, Haodan, Xu, S., Wei, C., Wang, S., Wang, Y., 2020. Distribution coefficients of trace metals between modern coral-lattices and seawater in the northern South China Sea: Species and SST dependencies. J. Asian Earth Sci. 187. https://doi.org/10.1016/j.jseaes.2019.104082

Johns, E.., Muhling, B.., Perez, R.., Müller-Karger, F.., Melo, N., Smith, R.., Lamkin, J.., Gerard, T.., Malca, E., 2014. Amazon River water in the northeastern Caribbean Sea and its effect on larval reef fish assemblages during April 2009. Fish. Oceanogr. 23, 472–494. https://doi.org/10.1111/fog.12082

Jones, R., Bessell-Browne, P., Fisher, R., Klonowski, W., Slivkoff, M., 2016. Assessing the impacts of

sediments from dredging on corals. Mar. Pollut. Bull. 102, 9–29. https://doi.org/10.1016/j.marpolbul.2015.10.049

KellerLynn, K., 2011. Buck Island Reef National Monument: geologic resources inventory report. Natural Resource Report NPS/NRSS/GRD/NRR—2011/462. Fort Collins, Colorado.

Kendall, M., Takata, L., Jensen, O., Hillis-Starr, Z., Monaco, M., 2005. Ecological Characterization of Salt River Bay National Historical Park and Ecological Preserve, U.S. Virgin Islands. NOAA Technical Memorandum NOS NCCOS 14.

Klochko, K., Kaufman, A.J., Yao, W., Byrne, R.H., Tossell, J.A., 2006. Experimental measurement of boron isotope fractionation in seawater. Earth Planet. Sci. Lett. 248, 276–285. https://doi.org/10.1016/j.epsl.2006.05.034

Krishna Kumar, S., Chandrasekar, N., Seralathan, P., 2010. Trace elements contamination in coral reef skeleton, gulf of Mannar, India. Bull. Environ. Contam. Toxicol. 84, 141–146. https://doi.org/10.1007/s00128-009-9905-3

Kuzminov, F.I., Brown, C.M., Fadeev, V. V, Gorbunov, M.Y., 2013. Effects of metal toxicity on photosynthetic processes in coral symbionts, Symbiodinium spp. J. Exp. Mar. Bio. Ecol. 446, 216–227. https://doi.org/10.1016/j.jembe.2013.05.017

Lane, C., Castillo II, B., 2017. Water chemistry, phytoplankton, and sediment dybnamics of nearshore habitats in Salt River Bay, St. Croix, USVI.

Larsen, E.H., Stürup, S., 1994. Carbon-enhanced inductively coupled plasma mass spectrometric detection of arsenic and selenium and its application to arsenic speciation. J. Anal. At. Spectrom. 9, 1099–1105.

LaVigne, M., Field, M.P., Anagnostou, E., Grottoli, A.G., Wellington, G.M., Sherrell, R.M., 2008. Skeletal P/Ca tracks upwelling in Gulf of Panamá coral: Evidence for a new seawater phosphate proxy. Geophys. Res. Lett. 35, 1–5. https://doi.org/10.1029/2007GL031926

Lea, D.W., Shen, G.T., Boyle, E.A., 1989. Coralline barium records temporal variability in equatorial Pacific upwelling. Nature 340, 373–376. https://doi.org/10.1038/340373a0

Li, H., Shi, A., Li, M., Zhang, X., 2013. Effect of pH, temperature, dissolved oxygen, and flow rate of overlying water on heavy metals release from storm sewer sediments. J. Chem. 2013. https://doi.org/10.1155/2013/434012

Li, Y.-H., Chan, L.-H., 1979. Desorptioni of Ba and Ra from river-borne sediments in the Hudson estuary. Earth Planet. Sci. Lett. 43, 343–350.

Long, E.R., Macdonald, D.D., Smith, S.L., Calder, F.D., 1995. Incidence of adverse biological effects within ranges of chemical concentrations in marine and estuarine sediments. Environ. Manage. 19, 81–97. https://doi.org/10.1007/BF02472006

Long, E.R., and Morgan, L.G., 1991. The potential for biological effects of sediment-sorbed contaminants tested in the National Status and Trends Program. NOAA Tech. Memo. NOS OMA 52. U.S. National Oceanic and Atmospheric Administration, Seattle, WA. 175 pp

Lorrain, A., Houlbrèque, F., Benzoni, F., Barjon, L., Tremblay-Boyer, L., Menkes, C., Gillikin, D.P., Payri, C., Jourdan, H., Boussarie, G., Verheyden, A., Vidal, E., 2017. Seabirds supply nitrogen to reef-building corals on remote Pacific islets. Sci. Rep. 7, 1–11. https://doi.org/10.1038/s41598-017-03781-y

Macdonald, J.I., Crook, D.A., 2010. Variability in Sr:Ca and Ba:Ca ratios in water and fish otoliths across an estuarine salinity gradient. Mar. Ecol. Prog. Ser. 413, 147–161. https://doi.org/10.3354/meps08703

Martín-Torre, M.C., Payán, M.C., Verbinnen, B., Coz, A., Ruiz, G., Vandecasteele, C., Viguri, J.R., 2015. Metal Release from Contaminated Estuarine Sediment under pH Changes in the Marine Environment. Arch. Environ. Contam. Toxicol. 68, 577–587. https://doi.org/10.1007/s00244-015-0133-z

May, L.A., Woodley, C.M., 2016. Phase I Porewater Toxicity Testing of Sediment from 25 Near-Shore Sites in St. Croix, USVI. NOAA NOS NCCOS CRCP Project 1133. Charleston, SC.

Miller, J., Muller, E., Rogers, C., Waara, R., Atkinson, A., Whelan, K.R.T., Patterson, M., Witcher, B., 2009. Coral disease following massive bleaching in 2005 causes 60% decline in coral cover on reefs in the US Virgin Islands. Coral Reefs 28, 925–937. https://doi.org/10.1007/s00338-009-0531-7

Mohammed, E.H., Wang, G., Jiang, J., 2010. The effects of nickel on the reproductive ability of three different marine copepods. Ecotoxicology 19, 911–916. https://doi.org/10.1007/s10646-010-0471-6

Mohammed, T.A.A.A., Dar, M.A., 2009. Ability of corals to accumulate heavy metals, northern red sea, Egypt. Environ. Earth Sci. 59, 1525–1534. https://doi.org/10.1007/s12665-009-0138-x

Mokhtar, M. Bin, Praveena, S.M., Aris, A.Z., Yong, O.C., Lim, A.P., 2012. Trace metal (Cd, Cu, Fe, Mn, Ni and Zn) accumulation in Scleractinian corals: A record for Sabah, Borneo. Mar. Pollut. Bull. 64, 2556–2563.

Moyer, R.P., Grottoli, A.G., Olesik, J.W., 2012. A multiproxy record of terrestrial inputs to the coastal ocean sing minor and trace elements (Ba/Ca, Mn/Ca, Y/Ca) and carbon isotopes ($\delta^{13}C$, $\Delta^{14}C$) in a nearshore coral from Puerto Rico. Paleoceanography 27, 1–14. https://doi.org/10.1029/2011PA002249

Muller, E.M., Rogers, C.S., Spitzack, A.S., Van Woesik, R., 2008. Bleaching increases likelihood of disease on *Acropora palmata* (Lamarck) in Hawksnest Bay, St John, US Virgin Islands. Coral Reefs 27, 191–195. https://doi.org/10.1007/s00338-007-0310-2

Muscatine, L., Goiran, C., Land, L., Jaubert, J., Cuif, J.-P., Allemand, D., 2005. Stable isotopes ($\delta^{13}C$ and $\delta^{15}N$) of organic matrix from coral skeleton. Proc. Natl. Acad. Sci. 102, 1525–1530.

Nahon, S., Richoux, N.B., Kolasinski, J., Desmalades, M., Pages, C.F., Lecellier, G., Planes, S., Lecellier, V.B., 2013. Spatial and temporal variations in stable carbon ($\delta^{13}C$) and nitrogen ($\delta^{15}N$) isotopic composition of symbiotic scleractinian corals. PLoS One 8, 1–17. https://doi.org/10.1371/journal.pone.0081247

National Marine Fisheries Service (NMFS), 2015. Recovery Plan for Elkhorn (*Acropora palmata*) and Staghorn (*A. cervicornis*) Corals. *Acropora* Recovery Team for the National Marine Fisheries Service, Silver Spring, MD. https://repository.library.noaa.gov/view/noaa/8950 (accessed 8-3-2020)

National Water Quality Monitoring Council, 2019. Water Quality Portal. https://www.waterqualitydata.us/portal/

Negri, A.P., Heyward, A.J., 2001. Inhibition of coral fertilisation and larval metamorphosis by tributyltin and copper. Mar. Environ. Res. 51, 17–27. https://doi.org/10.1016/S0141-1136(00)00029-5

Negri, A.P., Hoogenboom, M.O., 2011. Water contamination reduces the tolerance of coral larvae to thermal stress. PLoS One 6. https://doi.org/10.1371/journal.pone.0019703

Negri, A.P., Smith, L.D., Webster, N.S., Heyward, A.J., 2002. Understanding ship-grounding impacts on a coral reef: Potential effects of anti-foulant paint contamination on coral recruitment. Mar. Pollut. Bull. 44, 111–117. https://doi.org/10.1016/S0025-326X(01)00128-X

Nobi, E.P., Dilipan, E., Thangaradjou, T., Sivakumar, K., Kannan, L., 2010. Geochemical and geo-statistical assessment of heavy metal concentration in the sediments of different coastal ecosystems of Andaman Islands, India. Estuar. Coast. Shelf Sci. 87, 253–264. https://doi.org/10.1016/j.ecss.2009.12.019

Ohkouchi, N., Ogawa, N.O., Chikaraishi, Y., Tanaka, H., Wada, E., 2015. Biochemical and physiological bases for the use of carbon and nitrogen isotopes in environmental and ecological studies. Prog. Earth Planet. Sci. 2, 1–17. https://doi.org/10.1186/s40645-015-0032-y

Oliver, L.M., Fisher, W.S., Fore, L., Smith, A., Bradley, P., 2018. Assessing land use, sedimentation, and water quality stressors as predictors of coral reef condition in St. Thomas, U.S. Virgin Islands. Environ. Monit. Assess. 190, 1–16. https://doi.org/10.1007/s10661-018-6562-1

Oliver, L.M., Lehrter, J.C., Fisher, W.S., 2011. Relating landscape development intensity to coral reef condition in the watersheds of St. Croix, US Virgin Islands. Mar. Ecol. Prog. Ser. 427, 293–302. https://doi.org/10.3354/meps09087

Owens, N.J.P., Law, C.S., 1989. Natural variations in ^{15}N content of riverine and estuarine sediments. Estuar. Coast. Shelf Sci. 28, 407–416. https://doi.org/10.1016/0272-7714(89)90088-7

Pait, A.S., Hartwell, S.I., Mason, A.L., Warner, R.A., Jeffrey, C.F.G., Hoffman, A.M., Apeti, D.A., Galdo, F.R.J., Pittman, S.J., 2016. Chapter 4: An assessment of chemical contaminants, toxicity and benthic infauna in sediments from the St. Thomas East End Reserves (STEER). pp 75-117. In: Pait, A.S., Hartwell, S.I., Bauer, L.J., Apeti, D.A., Mason, A.L., 2016. An Integrated Environmental Assessment of the St. Thomas East End Reserves (STEER). NOAA Technical Memorandum NOS NCCOS 202. Silver Spring, MD, 219 pp

Patterson, C., Settle, D., Glover, B., 1976. Analysis of lead in polluted coastal seawater. Mar. Chem. 4, 305–319.

Patterson, K.L., Porter, J.W., Ritchie, K.B., Polson, S.W., Mueller, E., Peters, E.C., Santavy, D.L., Smith, G.W., 2002. The etiology of white pox, a lethal disease of the Caribbean elkhorn coral, *Acropora palmata*. Proc. Natl. Acad. Sci. 99, 8725–8730. https://doi.org/10.1073/pnas.092260099

Peterson, B.J., Fry, B., 1987. Stable Isotopes in Ecosystem Studies. Annu. Rev. Ecol. Syst. 18, 293–320. https://doi.org/10.1146/annurev.es.18.110187.001453

Pittman, S.J., Bauer, L., Hile, S.D., Jeffrey C.F.G., Davenport, E., Caldo, C., 2014. Marine Protected Areas of the US Virgin Islands: Ecological Performance Report. Silver Spring, MD.

Prouty, N.G., Hughen, K.A., Carilli, J., 2008. Geochemical signature of land-based activities in Caribbean coral surface samples. Coral Reefs 27, 727–742. https://doi.org/10.1007/s00338-008-0413-4

Rädecker, N., Pogoreutz, C., Voolstra, C.R., Wiedenmann, J., Wild, C., 2015. Nitrogen cycling in corals: The key to understanding holobiont functioning? Trends Microbiol. 23, 490–497. https://doi.org/10.1016/j.tim.2015.03.008

Rajkumar, W., Persad, D., 1994. Heavy metals and petroleum hydrocarbons in nearshore areas of Tobago, West Indies. Mar. Pollut. Bull. 28, 701–703. https://doi.org/10.1016/0025-326X(94)90306-9

Ramos, A.A., Inoue, Y., Ohde, S., 2004. Metal contents in Porites corals: Anthropogenic input of river run-off into a coral reef from an urbanized area, Okinawa. Mar. Pollut. Bull. 48, 281–294.

https://doi.org/10.1016/j.marpolbul.2003.08.003

Ratheesh Kumar, C.S., Joseph, M.M., Gireesh Kumar, T.R., Renjith, K.R., Manju, M.N., Chandramohanakumar, N., 2010. Spatial variability and contamination of heavy metals in the inter-tidal systems of a tropical environment. Int. J. Environ. Res. 4, 691–700.

Reichelt-Brushett, A.J., Harrison, P.L., 2005. The effect of selected trace metals on the fertilization success of several scleractinian coral species. Coral Reefs 24, 524–534. https://doi.org/10.1007/s00338-005-0013-5

Reichelt-Brushett, A.J., Harrison, P.L., 2004. Development of a sublethal test to determine the effects of copper and lead on scleractinian coral larvae. Arch. Environ. Contam. Toxicol. 47, 40–55. https://doi.org/10.1007/s00244-004-3080-7

Reichelt-Brushett, A.J., McOrist, G., 2003. Trace metals in the living and nonliving components of scleractinian corals. Mar. Pollut. Bull. 46, 1573–1582. https://doi.org/10.1016/S0025-326X(03)00323-0

Risk, M.J., Lapointe, B.E., Sherwood, O.A., Bedford, B.J., 2009. The use of δ^{15}N in assessing sewage stress on coral reefs. Mar. Pollut. Bull. 58, 793–802. https://doi.org/10.1016/j.marpolbul.2009.02.008

Rogers, C.S., 1979. The effects of shading on coral reef structure and function. J. Exp. Mar. Bio. Ecol. 41, 269–288.

Rogers, K.M., 2003. Stable carbon and nitrogen isotope signatures indicate recovery of marine biota from sewage pollution at Moa Point, New Zealand. Mar. Pollut. Bull. 46, 821–827. https://doi.org/10.1016/S0025-326X(03)00097-3

Sammarco, P.W., Risk, M.J., Schwarcz, H.P., Heikoop, J.M., 1999. Cross-continental shelf trends in coral δ^{15}N on the Great Barrier Reef: Further consideration of the reef nutrient paradox. Mar. Ecol. Prog. Ser. 180, 131–138. https://doi.org/10.3354/meps180131

Sanyal, A., Nugent, M., Reeder, R.J., Bijma, J., 2000. Seawater pH control on the boron isotopic composition of calcite: Evidence from inorganic calcite precipitation experiments. Geochim. Cosmochim. Acta 64, 1551–1555. https://doi.org/10.1016/S0016-7037(99)00437-8

Sbriz, L., Aquino, M.R., Alberto De Rodriguez, N.M., Fowler, S.W., Sericano, J.L., 1998. Levels of chlorinated hydrocarbons and trace metals in bivalves and nearshore sediments from the Dominican Republic. Mar. Pollut. Bull. 36, 971–979. https://doi.org/10.1016/S0025-326X(98)00097-6

Seemann, J., González, C.T., Carballo-Bolaños, R., Berry, K., Heiss, G.A., Struck, U., Leinfelder, R.R., 2013. Assessing the ecological effects of human impacts on coral reefs in Bocas del Toro, Panama. Environ. Monit. Assess. 186, 1747–1763. https://doi.org/10.1007/s10661-013-3490-y

Shah, S.B., 2008. Study of Heavy Metal Accumulation in Scleractinian Corals of Viti Levu, Fiji Islands. Master's Thesis. University of the South Pacific, Suva, Fiji Islands, 173 pp.

Shen, G.T., Boyle, E.A., Lea, D.W., 1987. Cadmium in corals as a tracer of historical upwelling and industrial fallout. Nature 328, 794–796.

Sigman, D.M., Karsh, K.L., Casciotti, K.L., 2009. Ocean Process Tracers: Nitrogen Isotopes in the Ocean. Encycl. Ocean Sci. 4138–4153.

Sinclair, D.J., Kinsley, L.P.J., McCulloch, M.T., 1998. High resolution analysis of trace elements in corals by laser ablation ICP-MS. Geochemica Cosmochim. Acta 62, 1889–1901.

Smith, L.D., Negri, A.P., Philipp, E., Webster, N.S., Heyward, A.J., 2003. The effects of antifoulant-paint-contaminated sediments on coral recruits and branchlets. Mar. Biol. 143, 651–657. https://doi.org/10.1007/s00227-003-1107-7

Sutherland, K.P., Shaban, S., Joyner, J.L., Porter, J.W., Lipp, E.K., 2011. Human pathogen shown to cause disease in the threatened eklhorn coral *Acropora palmata*. PLoS One 6, 1–7. https://doi.org/10.1371/journal.pone.0023468

Tessier, A., Campbell, P.G.C., Bisson, M., 1979. Sequential Extraction Procedure for the Speciation of Particulate Trace Metals. Anal. Chem. 51, 844–851.

Titlyanov, E.A., Kiyashko, S.I., Titlyanova, T. V., Kalita, T.L., Raven, J.A., 2008. δ^{13}C and δ^{15}N values in reef corals Porites lutea and P. cylindrica and in their epilithic and endolithic algae. Mar. Biol. 155, 353–361. https://doi.org/10.1007/s00227-008-1025-9

Turgeon, D.D., Asch, B.D., Causey, R.E., Dodge, R.E., Jaap, W., Banks, J., Delaney, B.D., Keller, R., Speiler, C.A., Matos, J.R., Garcia, E., Diaz, D., Catanzaro, D., Rogers, C., Hillis-Starr, Z., Nemeth, R., Taylor, M., Schmahl, G., Miller, M., Gulko, D., Maragos, J., Friedlander, A., Hunter, C., Brainard, R., Craig, P., Richond, R., Davis, G., Starmer, J., Trianni, M., Houk, P., Birkeland, C., Edward, A., Golbuu, Y., Gutierrez, J., Idechong, N., Paulay, G., Tafileichig, A., Vander Velde, N., 2002. The State of Coral Reef Ecosystems of the United States and Pacific Freely Associated States: 2002. Silver Spring, MD.

USDA, 1987. Soil Mechanics Level 1: Module 3 - USDA Textural Soil Classification.

Vargas-Ángel, B., Peters, E.C., Kramarsky-Winter, E., Gilliam, D.S., Dodge, R.E., 2007. Cellular reactions to sedimentation and temperature stress in the Caribbean coral Montastraea cavernosa. J. Invertebr. Pathol. 95, 140–145. https://doi.org/10.1016/j.jip.2007.01.003

Wang, X.T., Sigman, D.M., Cohen, A.L., Sinclair, D.J., Sherrell, R.M., Weigand, M.A., Erler, D. V., Ren, H., 2015. Isotopic composition of skeleton-bound organic nitrogen in reef-building symbiotic corals: A new method and proxy evaluation at Bermuda. Geochim. Cosmochim. Acta 148, 179–190. https://doi.org/10.1016/j.gca.2014.09.017

Weber, M., de Beer, D., Lott, C., Polerecky, L., Kohls, K., Abed, R.M.M., Ferdelman, T.G., Fabricius, K.E., 2012. Mechanisms of damage to corals exposed to sedimentation. PNAS Early Edition, 1–10.

Whitall, D., Mason, A., Pait, A., Brune, L., Fulton, M., Wirth, E., Vandiver, L., 2014. Organic and metal contamination in marine surface sediments of Guánica Bay, Puerto Rico. Mar. Pollut. Bull. 80, 293–301. https://doi.org/10.1016/j.marpolbul.2013.12.053

Whitall, D., Pait, A., Ian Hartwell, S., 2015. Chemical contaminants in surficial sediment in Coral and Fish Bays, St. John, U.S. Virgin Islands. Mar. Environ. Res. 112, 1–8. https://doi.org/10.1016/j.marenvres.2015.08.001

Yamamuro, M., Kayanne, H., Minagawa, M., 1995. Carbon and nitrogen stable isotopes of primary producers in coral reef ecosystems. Limnol. Oceanogr. 40, 617–621.

Supplementary Material

Supplementary Tables

Table S1. U.S. Virgin Islands water quality criteria. Class A waters should not exceed Class B water quality standards in any case. Listed are Class B and Class C water quality parameters that are evaluated by DPNR when determining if a water body meets the water quality criteria (USVI DPNR 2019).

Criterion Evaluated	**Class B**	**Class C**
Dissolved Oxygen	≥ 5.5 mg/l	≥ 5.0 mg/l
pH	≤ 8.3 to ≥ 7.0	≤ 8.5 to ≥ 6.7
Temperature	≤ 32° C; ≤ 29° C in coral reef ecosystems	Same as Class B
Total Phosphorus	Not to exceed 50 µg/L	Same as Class B
Total Nitrogen	Not to exceed 207 µg/L in > 10 % of samples over a three-year period	Same as Class B
Turbidity	A maximum NTU reading of 3 shall be permissible; should not exceed 1 NTU in coral reef ecosystems	Same as Class B
Secchi Depth	Visible at a minimum depth of 1 meter	Same as Class B
Bacteria	Enterococci shall not exceed 30 CFU/100 mL for the 30-day geometric mean; enterococci shall not exceed 110 CFU/100 mL in more than 10 % of samples collected within the same 30 days.	Same as Class B
Chlorine	The 4-day average concentration of Chlorine shall not exceed 7.5 µg/l. The 1-hour average concentration of Chlorine shall not exceed 13 µg/l	Same as Class B

Table S2. GPS coordinates of coral and sediment samples.

Coral Sites	**Latitude (DDM)**	**Longitude (DDM)**
SARI 1	N 17°46.873	W 64°44.707
SARI 2	N 17°47.003	W 64°45.180
SARI 3	N 17°46.824	W 64°45.268
BUIS 1	N 17°46.994	W 64°36.989
BUIS 2	N 17°47.241	W 64°36.576
BUIS 4	N 17°47.553	W 64°36.371
BUIS 6	N 17°47.767	W 64°36.639
Sediment Sites	**Latitude (DDM)**	**Longitude (DDM)**
SARI 1	N 17°46.873	W 64°44.707
SARI 2	N 17°47.003	W 64°45.180
SARI 3	N 17°46.824	W 64°45.268
SARI 4	N 17°46.521	W 64°45.260
SARI 5	N 17°46.682	W 64°45.237
SARI 6	N 17°46.358	W 64°45.180
SARI 7	N 17°46.490	W 64°45.234
SARI 8	N 17°46.054	W 64°45.584
SARI 9	N 17°46.356	W 64°45.608
SARI 10	N 17°46.564	W 64°45.557
SARI 11	N 17°46.499	W 64°45.666
SARI 12	N 17°46.852	W 64°45.893
BUIS 1	N 17°46.994	W 64°36.989
BUIS 2	N 17°47.241	W 64°36.576
BUIS 4	N 17°47.553	W 64°36.371

Table S3. Coral colony size and colony percent tissue mortality by site. Colony size (cm) is mean length in its longest dimension (SE = standard error).

Site	Colony length (cm)	± SE	Mortality (%)	± SE
SARI 1	87.2	7.9	25.0	7.1
SARI 2	132.0	25.3	31.0	6.1
SARI 3	128.5	18.6	20.5	4.4
BUIS 1	150.0	13.0	7.0	0.8
BUIS 2	155.5	8.7	19.5	3.9
BUIS 4	157.5	19.3	42.5	11.6

Table S4. 2017 water quality data compiled from the Water Quality Portal (https://www.waterqualitydata.us/portal/). Highlighted values exceed the class B water quality criteria for coral reef ecosystems shown in Table S1.

2017 Data	Temp °C	Salinity (ppt)	pH	DO (mg/l)	Total P (µg/l)	Kjeldahl N (µg/l)	Secchi Depth (m)	TSS (mg/L)	Turbidity (NTUs)	Enterococcus (MPN/100mL)
SARI Average	28.2	35.0	8.10	5.87	5.76	211	2.07	5.87	2.48	40
SARI Min	26.6	32.8	7.83	3.88	2.00	96	0.60	2.90	0.02	0
SARI Max	30.6	35.9	8.54	8.02	15.3	335	4.50	8.40	7.92	210
BUIS Average	27.7	35.3	8.05	6.29	3.62	0.44	3.82	3.99	0.29	<10
BUIS Min	26.6	33.9	7.97	6.03	1.70	<0.09	1.80	1.80	0.07	<1
BUIS Max	29.4	36.6	8.09	6.82	4.90	0.80	6.10	6.80	0.65	20

Table S5. Measured and assigned values for AIST Certified Geochemical Reference Material JCp-1 Coral (*Porites* sp.). Li, Al, and Zn are listed here but are not pictured in Figure S4 because the mass fraction ratio exceeds visibility on the chart. Highlighted values are non-certified informational values, and these comparisons do not account for any method biases in either the measured or assigned values. The uncertainty for the assigned value represents the 95 % confidence interval.

Element and Mode	Measured Value (µg/g)	± SE (µg/g)	Assigned Value (µg/g)	± Uncertainty (µg/g)
7 -> 7 Li [No Gas]	0.39	0.02	1.3	NA
11 -> 11 B [No Gas]	50.83	0.34	47.7	NA
23 -> 23 Na [He]	4038.53	62.0	4350	30
24 -> 24 Mg [He]	985.59	13.1	972	8
27 -> 27 Al [He]	30.64	1.45	480 - 490	NA
31 -> 47 P [O_2]	4.14	0.41	4.1	0.9
44 -> 44 Ca [He]	387081	10905	380000	NA
55 -> 55 Mn [He]	0.61	0.03	1	0.1
57 -> 57 Fe [He]	11.95	0.16	29	2
64 -> 64 Zn [He]	0.87	0.62	0.5	NA
88 -> 88 Sr [He]	7207.06	53.8	7240	70
114 -> 114 Cd [He]	0.026	0.004	0.028 - 0.032	NA
138 -> 138 Ba [He]	8.79	0.13	10.3	0.5

Table S6. Sediment trace element mass fractions by site. Mass fractions (µg/g dry mass fraction) are the mean from three replicates [± standard error]. Mg, Al, and Fe are listed as percentages [± standard error].

Site	Li	±SE	Be	±SE	B	±SE	Na	±SE	Mg %	±SE %	Al %	±SE %	K	±SE	V	±SE	Cr	±SE	Fe %	±SE %	Mn	±SE	Ni	±SE	Cu	±SE
SARI 1	1.59	0.07	0.04	0.01	38.3	2.75	8311	518	1.50	0.07	0.45	0.09	1090	140	5.69	0.97	3.45	0.24	0.22	0.04	76.2	10.9	1.46	0.14	1.59	0.22
SARI 2	1.54	0.28	0.03	< 0.01	30.1	2.13	6240	898	1.55	0.06	0.21	0.09	513	168	5.13	1.85	5.49	0.28	0.14	0.05	133	85.4	1.61	0.28	1.16	0.34
SARI 3	2.32	0.24	0.05	< 0.01	31.9	0.24	7504	101	1.41	0.02	0.55	0.01	978	46.2	6.94	0.15	4.49	0.13	0.22	< 0.01	98.9	7.87	1.51	0.03	1.57	0.14
SARI 4	3.83	0.46	0.02	0.02	12.8	12.8	10365	1010	1.40	0.04	0.78	0.03	1483	69.7	11.5	0.42	4.94	0.05	0.38	0.01	126	4.61	3.08	0.53	3.24	0.24
SARI 5	7.79	0.44	0.20	0.03	14.0	14.0	13669	656	1.64	0.03	2.76	0.25	4289	373	47.6	4.58	13.0	1.23	1.90	0.21	480	41.5	7.10	1.00	15.3	0.73
SARI 6	22.9	0.88	0.32	0.02	65.3	19.6	43955	2415	1.64	0.04	3.78	0.21	8692	264	65.2	2.27	30.3	0.58	2.55	0.09	309	8.90	19.5	1.18	41.2	0.93
SARI 7	3.31	0.33	0.05	0.01	9.53	9.53	11449	2141	1.54	0.02	0.69	0.11	1319	227	11.8	2.32	11.6	5.31	0.40	0.09	127	23.6	4.61	2.10	3.81	1.48
SARI 8	30.8	0.99	0.57	0.06	75.4	12.9	56817	2758	1.90	0.04	6.13	0.21	10584	39.3	103	4.25	34.3	1.14	3.76	0.09	382	0.60	24.6	1.83	82.2	2.97
SARI 9	10.7	0.06	0.50	0.07	6.20	6.20	20151	459	1.24	0.04	5.84	0.28	7163	281	115	5.70	34.6	6.66	4.23	0.25	789	39.9	19.4	1.09	52.4	3.38
SARI 10	4.39	0.34	0.12	0.03	11.1	11.1	15565	1058	1.03	0.01	1.19	0.04	2079	25.4	19.8	0.56	7.65	0.53	0.61	< 0.01	156	4.26	4.43	0.82	7.71	0.30
SARI 11	9.12	0.19	0.15	0.02	23.7	15.6	26726	434	0.99	< 0.01	2.56	0.07	3602	29.4	40.8	0.27	25.3	0.51	1.86	0.03	250	3.74	11.7	1.17	60.6	3.56
SARI 12	1.51	0.05	0.04	< 0.01	30.5	2.28	7591	675	1.74	0.02	0.35	0.05	769	87.9	6.59	1.26	3.59	0.39	0.20	0.03	73.8	9.69	1.27	0.12	1.90	0.34
BUIS 1	0.68	0.07	< 0.01	< 0.01	40.4	0.51	8006	418	0.81	0.04	0.01	< 0.01	285	20.4	0.37	0.04	2.32	0.12	0.01	< 0.01	6.23	0.25	0.65	0.01	0.24	0.02
BUIS 2	0.84	0.08	0.01	< 0.01	40.8	2.30	8744	249	1.22	0.02	0.01	< 0.01	408	23.3	0.55	0.01	3.17	0.06	0.01	< 0.01	17.0	0.30	0.96	0.06	0.81	0.21
BUIS 4	0.79	0.05	0.01	< 0.01	39.7	0.83	7330	235	1.15	0.02	< 0.01	< 0.01	255	13.4	0.27	0.01	2.66	0.05	< 0.01	< 0.01	11.8	0.59	0.71	0.04	0.27	0.03

Site	Zn	±SE	As	±SE	Se	±SE	Rb	±SE	Sr	±SE	Mo	±SE	Ag	±SE	Cd	±SE	Sb	±SE	Te	±SE	Ba	±SE	Tl	±SE	Pb	±SE
SARI 1	6.58	1.30	2.50	0.16	0.08	0.02	1.57	0.32	3649	105	0.11	0.01	0.02	< 0.01	0.03	< 0.01	0.07	0.01	0.01	< 0.01	45.9	11.7	0.02	< 0.01	1.53	0.02
SARI 2	3.28	1.29	3.27	1.21	0.07	0.03	0.73	0.30	3566	112	0.15	0.02	0.01	< 0.01	0.04	0.01	0.12	0.05	< 0.01	< 0.01	11.8	2.49	0.02	< 0.01	0.84	0.17
SARI 3	6.45	0.28	1.99	0.08	0.10	0.02	1.52	0.05	3945	57.4	0.21	0.01	0.02	< 0.01	0.03	< 0.01	0.12	0.01	< 0.01	< 0.01	32.2	0.85	0.05	< 0.01	0.89	0.01
SARI 4	17.2	2.40	2.21	0.59	0.32	0.32	2.81	0.05	4145	155	< 0.01	< 0.01	< 0.01	< 0.01	0.04	0.04	0.18	0.18	0.01	0.01	36.2	5.47	0.05	0.01	1.19	0.01
SARI 5	55.5	5.13	4.82	0.17	0.40	0.39	7.91	0.65	2875	100	< 0.01	< 0.01	0.11	0.08	0.05	0.03	0.36	0.36	0.18	0.05	108	9.22	0.11	0.01	3.27	0.30
SARI 6	64.6	3.49	11.1	1.29	1.16	0.39	20.1	0.49	2122	269	< 0.01	< 0.01	0.06	0.02	0.10	0.05	0.35	0.27	0.08	0.03	121	3.75	0.17	0.03	7.32	0.28
SARI 7	14.3	5.09	1.13	0.24	0.55	0.43	2.28	0.53	3999	81.8	< 0.01	< 0.01	0.01	0.01	0.02	0.01	0.11	0.11	0.06	0.05	29.4	6.13	0.02	0.01	1.18	0.32
SARI 8	83.5	5.31	2.40	0.45	3.56	1.01	24.5	0.94	187.3	9.77	< 0.01	< 0.01	0.10	0.01	0.15	0.07	0.27	0.27	0.02	0.01	182	5.44	0.27	0.02	20.2	0.36
SARI 9	147	25.7	2.37	0.32	0.43	0.34	14.3	0.56	1086	36.4	< 0.01	< 0.01	0.07	0.02	0.09	0.06	0.17	0.17	0.08	0.06	337	2.01	0.10	0.01	10.1	0.26
SARI 10	25.7	9.73	1.03	0.30	1.18	1.06	3.73	0.11	4728	35.7	< 0.01	< 0.01	0.02	0.02	0.03	0.02	0.12	0.12	0.02	0.01	57.8	1.60	0.07	0.01	1.47	0.04
SARI 11	68.0	1.32	5.56	0.30	0.93	0.52	7.63	0.02	3789	50.4	< 0.01	< 0.01	0.02	0.01	0.08	0.05	0.16	0.16	0.02	0.02	79.8	0.90	0.23	< 0.01	4.32	0.11
SARI 12	4.48	0.66	2.02	0.35	0.12	0.04	0.97	0.12	3222	115	0.13	0.04	0.02	< 0.01	0.03	< 0.01	0.03	< 0.01	0.01	0.01	26.8	5.76	0.02	< 0.01	0.99	0.12
BUIS 1	0.77	0.33	0.63	0.05	0.07	0.02	0.13	0.02	5790	72.9	0.10	< 0.01	0.01	< 0.01	0.01	< 0.01	0.02	< 0.01	< 0.01	< 0.01	8.60	0.45	< 0.01	< 0.01	0.23	0.01
BUIS 2	1.09	0.32	0.98	0.03	0.06	0.01	0.16	0.01	5144	144	0.20	< 0.01	0.02	0.01	0.01	< 0.01	0.02	< 0.01	< 0.01	< 0.01	9.57	0.63	0.01	< 0.01	0.52	0.02
BUIS 4	0.59	0.31	0.84	0.02	0.07	< 0.01	0.08	< 0.01	5287	87.5	0.17	0.05	0.01	< 0.01	0.01	< 0.01	0.01	< 0.01	< 0.01	< 0.01	7.56	0.20	0.01	< 0.01	0.32	0.01

Table S7. Mercury (Hg) mass fractions (ng/g dry mass fraction) in the sediment. Three sediment sample replicates were measured from each site with the mean mass fraction [± standard error] displayed for each site.

Site	Hg (ng/g)	± SE (ng/g)
SARI 1	5.50	0.48
SARI 2	1.67	0.49
SARI 3	2.45	0.02
SARI 4	4.20	0.83
SARI 5	9.70	0.63
SARI 6	43.64	2.80
SARI 7	3.30	0.59
SARI 8	56.00	1.79
SARI 9	28.81	9.93
SARI 10	5.77	0.05
SARI 11	28.62	1.40
SARI 12	0.71	0.01
BUIS 1	0.68	0.04
BUIS 2	0.97	0.08
BUIS 4	0.89	0.05

Table S8. Coral skeleton trace element mass fractions by site. Mass fractions (µg/g dry mass fraction) in the skeleton are shown as means from ten colonies at each site [± standard error]. Calcium is displayed as a percentage [± standard error].

Site	Li	±SE	B	±SE	Na	±SE	Mg	±SE	Al	±SE	P	±SE	Ca %	±SE %	V	±SE	Cr	±SE	Mn	±SE	Fe	±SE	Co	±SE	Ni	±SE
SARI 1	0.40	0.01	52.5	1.19	4073	97.8	1208	61	6.02	0.70	31.5	3.98	42.1	1.19	0.04	< 0.01	0.18	0.16	0.53	0.06	11.8	6.33	0.14	< 0.01	0.60	0.13
SARI 2	0.41	0.01	56.8	1.94	3903	67.2	1170	83	6.21	0.50	31.5	2.95	36.7	0.54	0.04	< 0.01	0.01	0.01	0.48	0.03	3.70	0.71	0.14	< 0.01	0.48	0.01
SARI 3	0.45	0.01	55.9	1.55	3941	31.5	1114	62	6.94	0.49	38.4	3.75	38.8	0.07	0.04	< 0.01	0.05	0.03	0.91	0.40	3.81	1.14	0.14	< 0.01	0.46	0.01
BUIS 1	0.39	0.02	61.5	3.60	4353	249	1245	146	8.12	2.27	56.2	17.3	39.0	2.78	0.04	< 0.01	0.01	0.01	0.55	0.13	3.79	1.39	0.14	0.01	0.48	0.06
BUIS 2	0.43	0.01	65.0	0.43	4152	58.1	1315	154	5.76	0.91	52.9	5.82	36.9	0.43	0.04	< 0.01	0.01	< 0.01	0.47	0.05	2.38	0.34	0.14	< 0.01	0.57	0.08
BUIS 4	0.40	0.01	62.8	1.88	4216	44.2	1230	87	7.07	1.56	51.5	14.2	39.0	2.00	0.04	< 0.01	0.08	0.06	0.46	0.07	5.74	2.36	0.14	0.01	0.55	0.07
BUIS 6	0.41	0.01	64.2	0.52	4300	37.3	1108	85	4.76	0.76	42.6	3.42	40.9	0.92	0.04	< 0.01	0.06	0.03	0.47	0.05	4.86	1.26	0.14	< 0.01	0.42	0.01

Site	Cu	±SE	Zn	±SE	Rb	±SE	Sr	±SE	Mo	±SE	Ag	±SE	Cd	±SE	Sb	±SE	Cs	±SE	Ba	±SE	Nd	±SE	Pb	±SE	U	±SE
SARI 1	0.22	0.06	3.32	0.95	0.01	< 0.01	7836	50.3	0.05	0.01	0.01	< 0.01	0.09	0.02	0.01	< 0.01	< 0.01	< 0.01	22.1	3.35	0.01	< 0.01	0.04	< 0.01	2.89	0.05
SARI 2	0.34	0.13	2.34	0.30	0.01	< 0.01	7617	42.2	0.16	0.08	0.01	< 0.01	0.07	0.01	0.02	< 0.01	< 0.01	< 0.01	19.4	2.93	0.01	< 0.01	0.04	< 0.01	2.79	0.08
SARI 3	0.20	0.03	4.63	0.61	0.01	< 0.01	7729	34.4	0.04	< 0.01	0.01	< 0.01	0.07	0.01	0.01	< 0.01	< 0.01	< 0.01	23.2	1.69	< 0.01	< 0.01	0.05	< 0.01	2.90	0.04
BUIS 1	0.14	0.03	2.91	2.29	0.01	< 0.01	7914	209	0.05	0.03	0.01	< 0.01	0.10	0.04	0.01	< 0.01	< 0.01	< 0.01	37.2	13.2	0.01	< 0.01	0.03	< 0.01	2.76	0.25
BUIS 2	0.24	0.07	1.15	0.32	0.01	< 0.01	7748	38.6	0.66	0.26	0.01	< 0.01	0.10	0.01	0.01	< 0.01	< 0.01	< 0.01	36.0	4.31	0.01	< 0.01	0.04	0.01	2.84	0.06
BUIS 4	0.19	0.03	1.87	0.82	0.01	< 0.01	7727	119	0.74	0.31	0.01	< 0.01	0.09	0.02	0.01	< 0.01	< 0.01	< 0.01	44.4	16.2	0.01	< 0.01	0.03	< 0.01	2.65	0.10
BUIS 6	0.15	0.02	0.91	0.20	0.01	< 0.01	7964	49.4	1.44	0.89	0.01	< 0.01	0.09	0.01	0.01	< 0.01	< 0.01	< 0.01	28.2	2.97	0.01	< 0.01	0.03	< 0.01	2.94	0.04

Table S9. Coral skeleton ratios of trace elements to calcium (X/Ca). Ratios are shown as means from ten colonies at each site (µmol/mol ± standard error).

Site	Li	±SE	B	±SE	Na	±SE	Mg	±SE	Al	±SE	P	±SE	Ca	±SE	V	±SE	Cr	±SE	Mn	±SE	Fe	±SE	Co	±SE	Ni	±SE
SARI 1	5.59	0.22	466	17.3	16910	339	4719	161	21.1	2.14	95.2	10.4	1E+06	0	0.08	0.004	0.30	0.27	0.90	0.08	18.8	9.80	0.49	0.01	0.95	0.19
SARI 2	6.53	0.18	574	13.8	18566	182	5295	422	25.2	2.02	111	10.9	1E+06	0	0.09	0.002	0.02	0.01	0.95	0.06	7.34	1.48	0.54	0.01	0.89	0.04
SARI 3	6.70	0.09	535	15.5	17730	164	4740	263	26.6	1.87	128	12.7	1E+06	0	0.08	0.003	0.10	0.07	1.72	0.74	7.06	2.11	0.52	0.01	0.81	0.02
BUIS 1	5.83	0.20	586	17.8	19476	342	5284	234	31.2	2.98	186	16.5	1E+06	0	0.08	0.002	0.02	0.01	1.02	0.07	6.92	0.74	0.53	0.02	0.85	0.05
BUIS 2	6.67	0.07	653	6.67	19601	197	5865	681	22.9	3.56	185	19.8	1E+06	0	0.09	0.004	0.02	0.01	0.93	0.10	4.59	0.65	0.55	0.01	1.06	0.15
BUIS 4	6.05	0.40	600	18.4	18979	824	5295	595	27.9	7.19	177	56.1	1E+06	0	0.08	0.005	0.14	0.10	0.87	0.15	10.2	3.72	0.52	0.04	0.99	0.15
BUIS 6	5.78	0.22	585	13.9	18406	284	4463	299	17.2	2.71	134	10.2	1E+06	0	0.08	0.002	0.12	0.06	0.83	0.07	8.45	2.09	0.50	0.02	0.71	0.02

Site	Cu	±SE	Zn	±SE	Rb	±SE	Sr	±SE	Mo	±SE	Ag	±SE	Cd	±SE	Sb	±SE	Cs	±SE	Ba	±SE	Nd	±SE	Pb	±SE	U	±SE
SARI 1	0.33	0.09	4.70	1.28	0.006	<0.001	8560	190	0.05	0.004	0.005	<0.001	0.07	0.01	0.01	0.001	3.4E-05	1.5E-05	15.0	1.96	0.006	0.002	0.02	0.001	1.16	0.04
SARI 2	0.59	0.24	3.97	0.55	0.009	0.001	9519	105	0.18	0.08	0.006	0.001	0.07	0.01	0.01	0.002	6.1E-05	2.5E-05	15.3	2.23	0.005	0.001	0.02	0.001	1.28	0.02
SARI 3	0.32	0.05	7.33	0.96	0.008	<0.001	9124	43.8	0.04	0.002	0.006	<0.001	0.07	0.008	0.01	0.001	2.9E-06	2.9E-06	17.5	1.29	0.003	0.001	0.03	0.001	1.26	0.02
BUIS 1	0.23	0.02	4.39	1.04	0.009	0.001	9299	141	0.06	0.01	0.005	<0.001	0.09	0.01	0.01	0.001	9.1E-05	1.8E-05	28.0	3.23	0.006	0.001	0.02	0.001	1.19	0.02
BUIS 2	0.41	0.12	1.88	0.52	0.010	0.001	9604	91.3	0.75	0.30	0.005	0.001	0.09	0.01	0.01	0.001	6.2E-05	3.4E-05	28.3	3.19	0.006	0.002	0.02	0.003	1.29	0.02
BUIS 4	0.32	0.07	2.83	1.11	0.008	0.001	9116	311	0.76	0.30	0.006	<0.001	0.08	0.03	0.01	0.001	4.3E-05	2.9E-05	34.8	14.0	0.005	0.003	0.02	0.002	1.15	0.03
BUIS 6	0.23	0.03	1.34	0.28	0.008	0.001	8949	157	1.41	0.85	0.005	<0.001	0.08	0.01	0.01	0.001	5.5E-05	2.4E-05	19.9	1.79	0.006	0.001	0.02	0.001	1.22	0.02

Table S10. Methodology used for coral skeleton trace element analysis associated with results shown in Table 4 (SRM/RM = standard reference material/reference material; NS = not specified; NA = not any; AAS = atomic absorption spectroscopy; ICP-AES = inductively coupled plasma – atomic emission spectroscopy; ICP-MS = inductively coupled plasma – mass spectrometry).

	Procedural Blanks	Internal Standard	SRM/RM	Tissue Removal	Skeletal Grinding	Pre-Digestion Rinse	Acid Digestion	Method
1	NS	NS	Yes	5 % NaClO 24 hr	After tissue removal	NA	HCl, (5:1) HNO_3-$HClO_4$ + heat	AAS
2	NS	NS	NS	Water pick	After tissue removal	Extensive cleaning w/acid	34 % HNO_3, HNO_3 conc, 36 % H_20_2, HCl conc.; filtered 20 µm	ICP-AES
3	Yes*	Yes	NS	2 % $C_6H_{11}NO_7$, sonication, water pick	After tissue removal	NA	(1:1) HNO_3-H_2O_2, HCl + heat	ICP-MS
4	Yes	Yes	Yes	5 % NaClO	After tissue removal	Unclear**	HNO_3 conc, microwave, filtered at 0.45 µm	AAS
5	Yes	Yes	Yes	10 % H_2O_2, sonication	After tissue removal	NA	2 % HNO_3	ICP-MS
6	Yes	Yes	Yes	5.65 - 6.0 % NaClO	Prior to tisue removal	NA	2 % HNO_3	ICP-MS

Sources: [1]Guzman and Jimenez, 1992; [2]Bastidas and Garcia, 1999; [3]Reichelt-Brushett and McOrist, 2003; [4]Mokhtar *et al.,* 2012; [5]Jiang *et al.,* 2020; [6]Current Study. *It is unclear whether these are procedural or instrument blanks. **Study cited extensive cleaning procedure but only mentioned crushing the skeleton.

Supplementary Figures

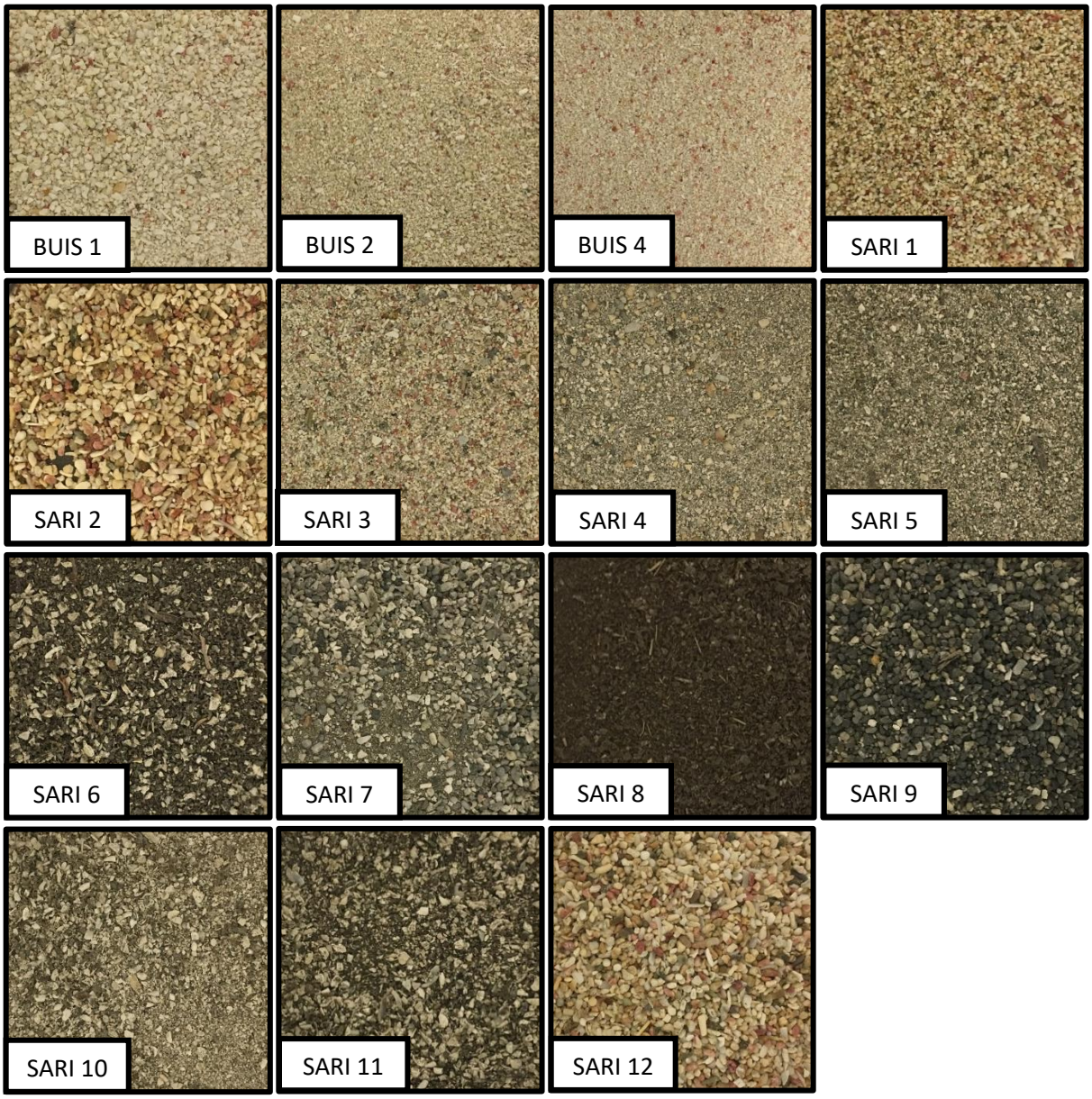

Figure S1. Sieved sediment sample images. Sediment samples are representative of the three replicates of sieved sediment (≤ 1 mm) from each site.

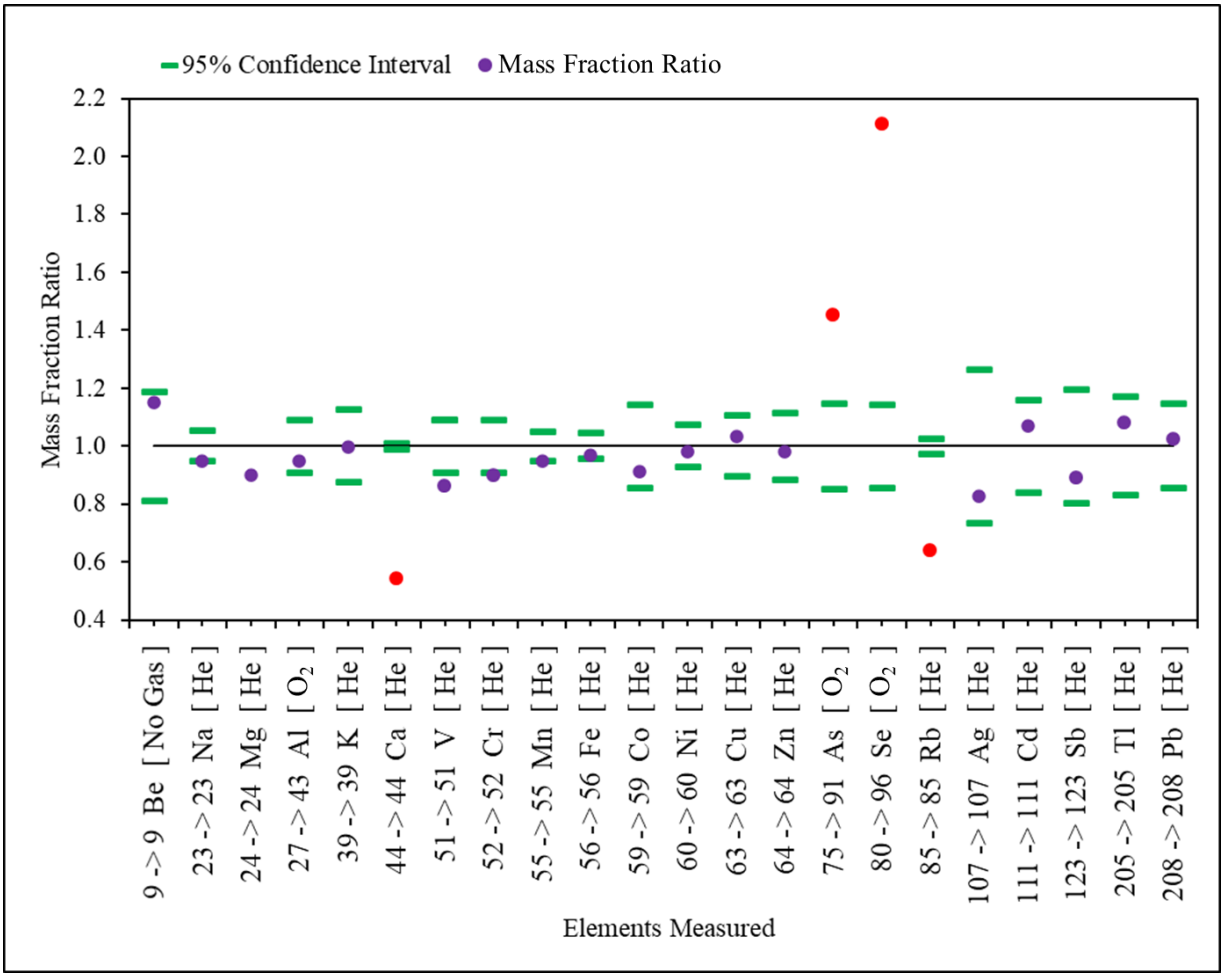

Figure S2. NIST SRM 1944. Measurements were made on NIST Standard Reference Material 1944 New York/New Jersey Waterway Sediment and compared to the assigned values. The assigned values include certified (Al, Cr, Mn, Fe, Ni, Zn, As, Cd, Pb), reference (Be, Na, K, Ca, V, Co, Cu, Se, Rb, Ag, Sb, Tl) and information values (Mg). Mass fraction ratios (measured value/assigned value) are shown in purple where the data fall within ± 20 % of the assigned values, or ratios are shown in red if outside of this range. The mass transitions and gas mode are given for QQQ-ICP-MS.

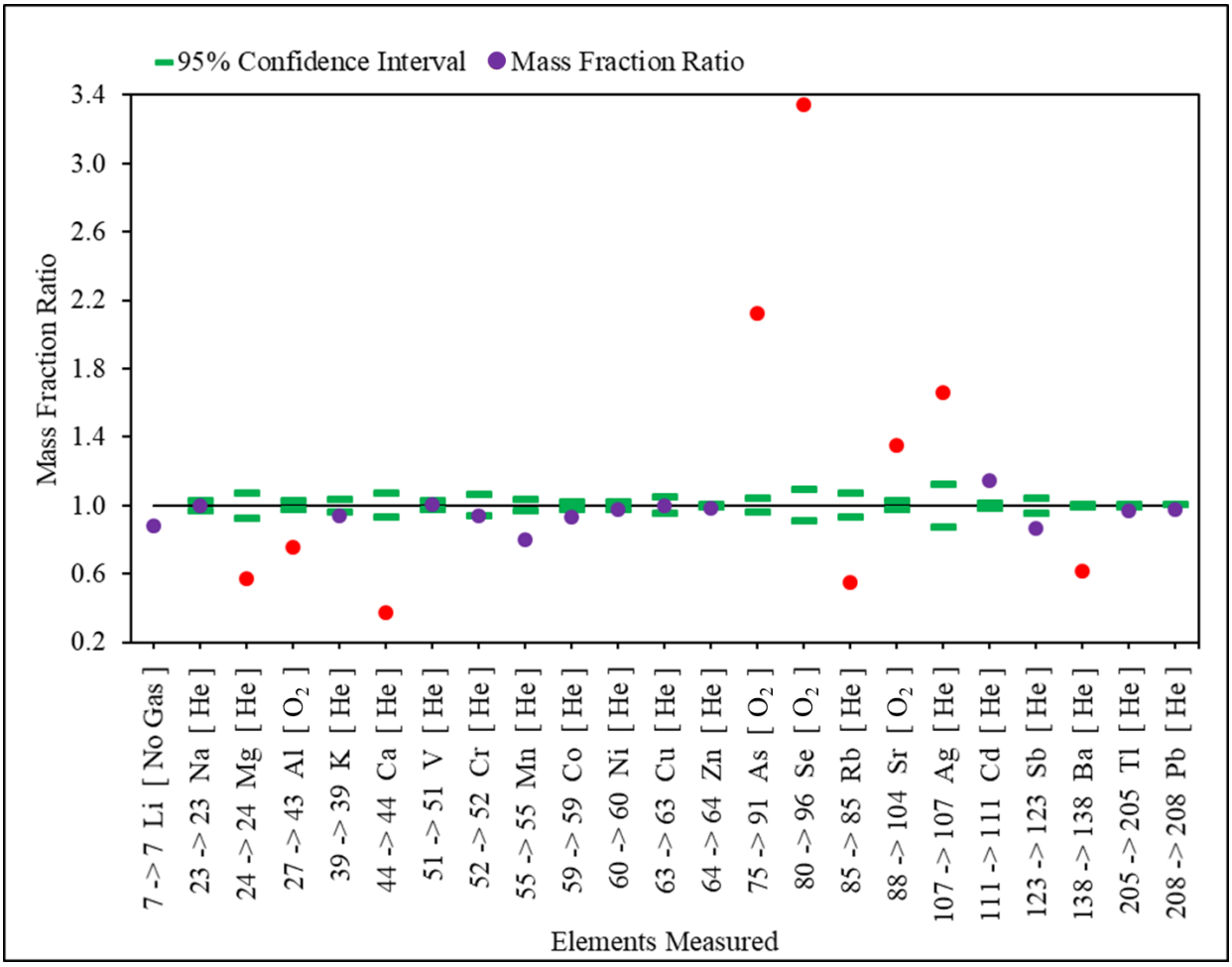

Figure S3. NIST SRM 2702. Measurements were made on NIST Standard Reference Material 2702 Inorganics in Marine Sediment and compared to the assigned values. The assigned values include certified (Na, Al, K, V, Cr, Mn, Co, Ni, Zn, As, Se, Rb, Sr, Cd, Sb, Ba, Tl, Pb), reference (Mg, Ca, Cu, Se, Ag) and information values (Li). Mass fraction ratios (measured value/assigned value) are shown in purple where the data fall within ± 20 % of the assigned values, or ratios are shown in red if outside of this range. The mass transitions and gas mode are given for QQQ-ICP-MS.

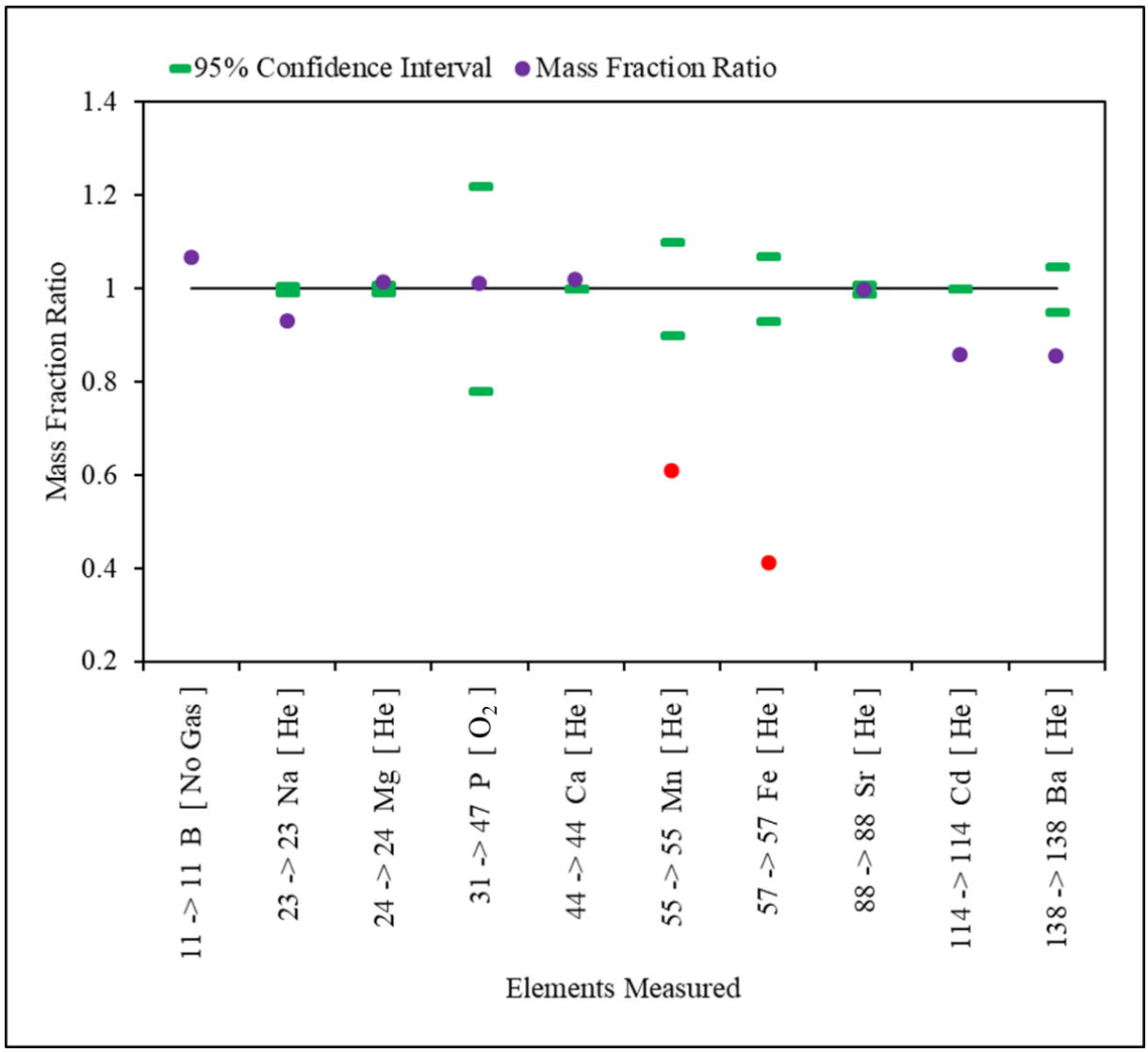

Figure S4. AIST SRM JCp-1. Measurements were made on AIST Certified Geochemical Reference Material JCp-1 Coral (*Porites* sp.) and compared to the assigned values. The assigned values include certified (Na, Mg, P, Ca, Mn, Fe, Sr, Ba) and information values (B, Cd) (See certificate: https://gbank.gsj.jp/geostandards/Certificate/PDF/eJCp1.pdf). Mass fraction ratios (measured value/assigned value) are shown in purple where the data fall within ± 20 % of the assigned values, or ratios are shown in red if outside of this range. The mass transitions and gas mode are given for QQQ-ICP-MS.